Weight-Constrained Sparse Arrays For Direction of Arrival Estimation Under High Mutual Coupling

Pranav Kulkarni, *Student Member, IEEE* and P. P. Vaidyanathan, *Life Fellow, IEEE*

***Abstract*—In recent years, following the development of nested arrays and coprime arrays, several improved array constructions have been proposed to identify $\mathcal{O}(N^2)$ directions with N sensors and to reduce the impact of mutual coupling on the direction of arrival (DOA) estimation. However, having $\mathcal{O}(N^2)$ degrees of freedom may not be of interest, especially for large N. Also, a large aperture of such arrays may not be suitable when limited space is available to place the sensors. This paper presents two types of sparse array designs that can effectively handle high mutual coupling by ensuring that the coarray weights satisfy either $w(1) = 0$ or $w(1) = w(2) = 0$, where $w(l)$ is the number of occurrences of the difference l in the set $\{n_i - n_j\}_{i,j=1}^{N}$, and n_i are sensors locations. In addition, several other coarray weights are small constants that do not increase with the number of sensors N. The arrays of the first type have an aperture of $\mathcal{O}(N)$ length, making them suitable when the available aperture is restricted and the number of DOAs is also $\mathcal{O}(N)$. These arrays are constructed by appropriately dilating a uniform linear array (ULA) and augmenting a few additional sensors. Despite having an aperture of $\mathcal{O}(N)$ length, these arrays can still identify more than N DOAs. The arrays of the second type have $\mathcal{O}(N^2)$ degrees of freedom and are suitable when the aperture is not restricted. These arrays are constructed by appropriately dilating a nested array and augmenting it with several additional sensors. We compare the proposed arrays with those in the literature by analyzing their coarray properties and conducting several Monte-Carlo simulations. Unlike ULA and nested array, any sensor pair in the proposed arrays has a spacing of at least 2 units, because of the coarray hole at lag 1. In the presence of high mutual coupling, the proposed arrays can estimate DOAs with significantly smaller errors when compared to other arrays because of the reduction of coarray weight at critical small-valued lags.**

***Index Terms*—Sparse arrays, $\mathcal{O}(N)$ aperture arrays, difference coarray, DOA estimation, mutual coupling, weight-constrained sparse arrays, weight-constrained nested arrays.**

I. Introduction

ARRAY signal processing has been a field of active research for several decades now [1]. In particular, direction of arrival (DOA) estimation is an important application of sensor arrays in many domains, such as wireless communications, radar, and astronomy. A linear integer array of N sensors

$$\mathbf{z} = \begin{bmatrix} n_1 & n_2 & \dots n_N \end{bmatrix}, \tag{1}$$

is used to identify the angles $\theta_1, \theta_2, \dots, \theta_D$ from which the D source signals impinge on the array. The difference coarray $\mathbb{D}_{\mathbf{z}} = \{n_i - n_j\}_{i,j=1}^{N}$ is the set of all differences between the sensor locations, and the coarray weights $w(l)$ denote the number of sensor pairs with distance l between them, i.e.

$$w(l) = |\{(i,j) \text{ where } n_i - n_j = l\}| \tag{2}$$

where $|\cdot|$ denotes the cardinality of the set. It is well-known that if the sources are uncorrelated, well-designed sparse arrays can identify up to $\mathcal{O}(N^2)$ DOAs through the 'difference coarray domain'. Minimum redundancy arrays (MRAs) [2] have long been recognized to achieve this. However, finding optimal MRA requires an exhaustive search, and tabulated sensor positions are available for only a small number of sensors [2], [3], [4]. The introduction of nested arrays [5] and coprime arrays [6], which have closed-form expressions for sensor locations, has opened up a new direction for research in the design of sparse arrays. Although nested arrays and coprime arrays can identify fewer DOAs than an MRA with the same number of sensors, their closed-form expression for sensor positions for any N makes them more practical and attractive.

A. Array Design Criteria and Their Drawbacks

Following the development of nested arrays and coprime arrays, several generalizations of these arrays, such as generalized coprime arrays [7] and improved nested arrays [8], have been proposed. Several extensions of these arrays including super nested arrays [9], [10], augmented nested arrays [11], dilated nested arrays [12], MISC arrays [13], thinned coprime arrays [14], and padded coprime arrays [15] have also been advanced. The design of these arrays is based on three key principles:

1) Sensor locations should be easily describable using a closed-form expression or simple generation rules.
2) The difference coarray of the array should have a long central ULA segment, typically of $\mathcal{O}(N^2)$ length.
3) The number of sensor pairs with small separations should be kept to a minimum.

The closed-form expression for sensor locations (criterion 1) is necessary to create arrays easily for any given number of sensors N. The large central ULA segment of $\mathcal{O}(N^2)$ length in the coarray (criterion 2) is enforced to ensure that the arrays can identify a large number of DOAs using coarray-based DOA

Received 12 January 2024; revised 8 June 2024 and 11 August 2024; accepted 12 September 2024. Date of publication 17 September 2024; date of current version 14 October 2024. This work was supported in part by the Office of Naval Research under Grant N00014- 21-1-2521 and in part by California Institute of Technology. The associate editor coordinating the review of this article and approving it for publication was Dr. Zai Yang. *(Corresponding author: Pranav Kulkarni.)*

The authors are with the Department of Electrical Engineering, California Institute of Technology, Pasadena, CA 91125 USA (e-mail: pkulkarn@caltech.edu; ppvnath@systems.caltech.edu).

Digital Object Identifier 10.1109/TSP.2024.3461720

TABLE I
KEY CRITERIA CONSIDERED FOR SPARSE ARRAY DESIGN, THEIR DRAWBACKS, AND MODIFICATIONS CONSIDERED IN THIS PAPER

Array Design Criteria	Drawback of the Criterion	Modification to the Criterion	Drawback for the Modification
Closed-form expression or simple rule for sensor positions	Can identify fewer DOAs than MRA with coarray-MUSIC	None	-
Central ULA segment of length $\mathcal{O}(N^2)$ in coarray	$\mathcal{O}(N^2)$ aperture may not be suitable, and $\mathcal{O}(N^2)$ DOFs may not be needed for large N	$\mathcal{O}(N)$ aperture sparse arrays having ULA segment of $\mathcal{O}(N)$ length in their coarray	Can identify only up to $\mathcal{O}(N)$ DOAs
$w(l)$ small but non-zero for $l = 1, 2, 3$	Not robust to high mutual coupling	$w(1) = 0$ or $w(1) = w(2) = 0$	Can identify fewer DOAs due to one-sided ULA segment in coarray

estimation algorithms such as coarray-MUSIC [5], [16], [17] and coarray-ESPRIT [18]. However, such a large coarray means that the array aperture will also be $\mathcal{O}(N^2)$, which may not be practical when a large number of sensors N is used. It is becoming more common to use almost a hundred sensors for large antenna arrays and massive MIMO in 6G technology [19], [20]. With such a large number of sensors, it may no longer be necessary for the arrays to have the capability to identify $\mathcal{O}(N^2)$ sources because the number of DOAs is typically not that large. In practical situations where the arrays are deployed, such as in smartphones and self-driving cars, there may be physical constraints on the array aperture. In such cases with aperture constraints, an $\mathcal{O}(N^2)$ aperture may not be of interest or desirable.

The third criterion above is to reduce the impact of mutual coupling between sensors [9], [21], [22] on DOA estimation. The exact impact of mutual coupling on the array output is unknown to the user and can be difficult to model precisely. However, the sensor pairs with small separations contribute the most to the mutual coupling. Thus, to reduce the effect of mutual coupling on DOA estimation error, the coarray weights for small lags such as $w(1), w(2)$, and $w(3)$ that contribute the most to the effect of mutual coupling are kept to a minimum (criterion 3). However, in order to ensure that the difference coarray of the array has a large *central* ULA segment, these weights are still non-zero. Even though some extensions of coprime arrays, such as extended padded coprime array [15] and thinned coprime array [14], can already achieve $w(1) = w(2) = w(3) = 1$, the presence of high mutual coupling may still result in poorer DOA estimation because of non-zero $w(1)$, $w(2)$, and $w(3)$.

To summarize, when dealing with arrays that have a large number of sensors, we can relax the requirement of having $\mathcal{O}(N^2)$ degrees of freedom (DOFs). Instead, other practical considerations, such as aperture constraint and robustness to high mutual coupling, become a priority. To address these requirements, we consider modifications to the second and third array design criteria in this paper and accordingly design sparse arrays. Table I summarizes the modifications made and their advantages and disadvantages. Sparse arrays with a closed form for sensor positions, such as nested arrays and coprime arrays, can identify fewer DOAs compared to MRAs. However, they became popular because of the practical benefit of having closed-form sensor locations (criterion 1) for any number of sensors. By making modifications to the other two design criteria as described in Table I, we further sacrifice the maximum number of identifiable DOAs, but in turn, achieve practical benefits such as improved robustness to high mutual coupling and suitability under aperture constraint.

B. Our Contributions and Connections to Literature

Adhering to the modified array design criteria, we first develop several sparse and weight-constrained arrays that have $\mathcal{O}(N)$ aperture and either $w(1) = 0$ or $w(1) = w(2) = 0$. These constructions are based on appropriately dilating a uniform linear array (ULA) and augmenting it with a few additional sensors. The *one-sided* ULA segments in the difference coarrays of these arrays start either from lag $l = 2$ or $l = 3$, and the coarrays have only a few holes. Since these arrays have an $\mathcal{O}(N)$ aperture, we can use more sensors than $\mathcal{O}(N^2)$ aperture arrays when there is a fixed aperture constraint. These arrays are better suited when the aperture is constrained, the number of DOAs D is $\mathcal{O}(N)$, and high mutual coupling is present. One may wonder why we cannot use an N-sensor uniform linear array (ULA) instead of the proposed $\mathcal{O}(N)$ aperture arrays. This is because DOA estimation using ULA can suffer significantly in the presence of mutual coupling due to the densely packed sensors. Furthermore, an N-sensor ULA can identify only up to $N - 1$ DOAs, whereas the proposed $\mathcal{O}(N)$ aperture arrays can identify $D > N$ DOAs (such as $D = 2N$) through the difference coarray domain, although these arrays no longer have $\mathcal{O}(N^2)$ degrees of freedom.

Next, for the situation where robustness to high mutual coupling is needed but the array aperture is not constrained, we propose another type of sparse and weight-constrained arrays. These arrays have either $w(1) = 0$ or $w(1) = w(2) = 0$ and $\mathcal{O}(N^2)$ degrees of freedom. We achieve this by suitably dilating a nested array and appending it with several extra sensors. The one-sided ULA segment in the difference coarray of these arrays starts either from $l = 2$ or $l = 3$ and has $\mathcal{O}(N^2)$ length. Through Monte-Carlo simulations, we demonstrate that in certain situations, our proposed arrays, having $\mathcal{O}(N^2)$ aperture and $\mathcal{O}(N^2)$ degrees of freedom, can outperform arrays proposed in the literature. Please note that the proposed arrays do not have a *central* ULA segment in their difference coarrays (because $w(1) = 0$), unlike many other well-known sparse arrays. However, we can still apply a modified coarray root-MUSIC on the one-sided ULA segment of the coarray. It is important to note that using a one-sided ULA segment from the coarray reduces the number of identifiable DOAs using coarray-MUSIC

compared to the case when there exists a central ULA segment in the coarray.

We now explain the novelty of our contributions in light of what is already known about sparse arrays. To the best of our knowledge, $\mathcal{O}(N)$ aperture arrays that can identify more DOAs than the number of sensors have not been systematically developed, or even mentioned in the literature before. Furthermore, to the best of our knowledge, all simulations in earlier papers considered a fixed number of sensors N. Instead of only comparing different array geometries for a fixed number of sensors N, we also propose comparing different array geometries under a fixed aperture constraint. This can be called 'aperture-constrained' evaluation of sensor arrays. To achieve good performance under such aperture-constrained setting, 'aperture-aware' design of sparse arrays is required. One way to do this is to explicitly impose a strict constraint on the array aperture in the design stage. In this paper, we take a different approach and propose a class of array geometries with a smaller $\mathcal{O}(N)$ aperture instead of a large $\mathcal{O}(N^2)$ aperture. Because of this, the proposed $\mathcal{O}(N)$ aperture arrays can be more suitable than many other arrays from the literature under the aperture constraint. In summary, motivated by practical aperture constraints that certain applications may require, we propose an 'aperture-constrained' evaluation of sensor arrays and an 'aperture-aware' design approach, through this paper. Such designs can be more practically useful than the large $\mathcal{O}(N^2)$ aperture arrays for certain applications.

Similarly, arrays with $w(1) = 0$ or $w(1) = w(2) = 0$ are not very common in the literature. The CADiS array proposed in [7] is one such sparse array construction with a closed form for sensor locations and $w(l) = 0$ for small values of l such as $1, 2, 3$, etc. However, CADiS arrays are not available for certain numbers of sensors (such as 17, 23, and 29) [14]. Furthermore, under aperture constraint, it may not be easy to come up with the design parameters (integers M, N, and p from [7] such that M and N are coprime and p is a divisor of M). Additionally, some of our proposed arrays with $\mathcal{O}(N^2)$ aperture can identify more DOAs than CADiS with coarray-MUSIC, as we will see. This is because the one-sided ULA segment in the difference coarray of CADiS does not start immediately after a few initial holes, unlike the proposed arrays. Another array construction called generalized nested array (GNA) [23] includes CADiS arrays as their special case and shares the property that $w(l) = 0$ for small values of l. Similar to the CADiS array, it may not be easy to decide design parameters (coprime integers α and β from [23]), especially under aperture constraint. Some arrays tabulated in [3] also have $w(1) = 0$, but these are obtained through an elaborate search and do not have closed-form expressions for sensor positions. The tabulation is available only for $N \leq 20$.

Some of the $\mathcal{O}(N)$ aperture arrays described in this work were presented in our conference paper [24]. This journal paper introduces several new arrays, presents extensive simulations over and beyond [24], and provides a thorough comparison with the arrays from the literature. The new contributions (and outline) of this journal paper are as follows:

1) We discuss the drawbacks of the sparse array design criteria and motivate modifications proposed in Table I (Sec. I-A).
2) We describe and justify the application of coarray-MUSIC to a one-sided ULA segment in coarray (Sec. III).
3) We introduce new $\mathcal{O}(N)$ aperture arrays with $w(1) = w(2) = 0$ that can perform better than the $\mathcal{O}(N)$ aperture arrays with $w(1) = 0$ proposed in [24] (Sec. IV-C, IV-D).
4) We propose $\mathcal{O}(N^2)$ aperture arrays with $w(1) = 0$ (Sec. V-A) or $w(1) = w(2) = 0$ (Sec. V-B).
5) We compare the coarray properties and coarray-MUSIC spectra of the proposed arrays with several arrays from the literature (Sec. VI-A). We present extensive Monte-Carlo simulations under two simulation settings (fixed N (Sec. VI-B) and fixed aperture A (Sec. VI-C)) to thoroughly compare different arrays, and discuss when we can expect the proposed arrays to perform well (Sec. VI-E).

Notations. Boldface letters such as $\mathbf{A}$ and $\mathbf{a}$ are used to denote matrices and vectors. $[\mathbf{A}]_{mn}$ denotes the (m, n)-th entry of $\mathbf{A}$. The k-th column of matrix $\mathbf{A}$ is denoted by $\mathbf{A}(:, k)$. The statistical expectation operator is denoted by $\mathbb{E}(\cdot)$. The notation $[[n_1, n_2]]$ is used to denote the set of integers n s.t. $n_1 \leq n \leq n_2$. The union of two sets $\mathbb{P}_1$ and $\mathbb{P}_2$ is denoted by $\mathbb{P}_1 \cup \mathbb{P}_2$. For a set $\mathbb{P}$, $\alpha\mathbb{P}$ is the set formed by multiplying each element in $\mathbb{P}$ by α, whereas $\mathbb{P} + \alpha$ is the set formed by adding α to each element in $\mathbb{P}$. The standard big-O notation is denoted by $\mathcal{O}(\cdot)$. The largest integer not greater than x is $\lfloor x \rfloor$, and the smallest integer not smaller than x is $\lceil x \rceil$. Rounding operation $\mathrm{round}(x)$ returns the integer closest to x.

II. Preliminaries

In this section, we summarize the signal model for DOA estimation, the effect of mutual coupling, and coarray-based DOA estimation. We consider the problem of estimating directions $\theta_1, \ldots, \theta_D$ of D monochromatic, far-field, uncorrelated sources. The half wavelength distance $\lambda/2$ is assumed to be unity without loss of generality. We also assume that D is known. For the array in Eq. (1), the array output $\mathbf{x}$ is modeled as [25]

$$\mathbf{x}[k] = \mathbf{A}\mathbf{s}[k] + \mathbf{n}[k], \tag{3}$$

where $\mathbf{A} = \begin{bmatrix}\mathbf{a}(\omega_1) & \mathbf{a}(\omega_2) & \ldots & \mathbf{a}(\omega_D)\end{bmatrix}$ is the array manifold matrix containing steering vectors $\mathbf{a}(\omega_i) = \begin{bmatrix}e^{j\omega_i n_1} & e^{j\omega_i n_2} & \ldots & e^{j\omega_i n_N}\end{bmatrix}^T$ corresponding to the D DOAs. Here, the physical DOAs θ_i are converted into corresponding ω-domain quantities $\omega_i = \pi \sin\theta_i$ for mathematical convenience. $\mathbf{s}[k]$ is the source amplitude vector, and $\mathbf{n}[k]$ is the additive Gaussian noise term. The sampled array outputs $\mathbf{x}[k]$ for $k = 1, \ldots, K$ are called snapshots. The output covariance matrix is estimated using K snapshots as

$$\widehat{\mathbf{R}}_x = \frac{1}{K}\sum_{k=1}^{K}\mathbf{x}[k]\mathbf{x}^H[k]. \tag{4}$$

For finite snapshots, $\widehat{\mathbf{R}}_x$ is only an approximation to the ideal coarray covariance matrix

$$\mathbf{R}_x = \mathbb{E}(\mathbf{x}\mathbf{x}^H) = \mathbf{A}\mathbf{P}\mathbf{A}^H + \sigma_n^2\mathbf{I}. \tag{5}$$

As the sources are uncorrelated, the source covariance matrix $\mathbf{P}$ is a diagonal matrix containing source powers $p_i = \mathbb{E}(\mathbf{s}_i \mathbf{s}_i^H) > 0$, and σ_n^2 is the noise variance. The signal-to-noise ratio (SNR) is defined as $\bar{\mathbf{p}}/\sigma_n^2$, where $\bar{\mathbf{p}} = \sum_{i=1}^{D} p_i/D$ is the average source power. Subspace-based DOA estimation algorithms such as MUSIC [16] and root-MUSIC [26] are based on the eigendecomposition of $\widehat{\mathbf{R}}_x$:

$$\widehat{\mathbf{R}}_x = \widehat{\mathbf{E}}\widehat{\mathbf{\Lambda}}\widehat{\mathbf{E}}^H \tag{6}$$

where $\widehat{\mathbf{\Lambda}}$ is a diagonal matrix with eigenvalues ordered in decreasing order of magnitude and $\widehat{\mathbf{E}}$ contains the corresponding eigenvectors. The last $N - D$ columns of $\widehat{\mathbf{E}}$ provide an approximation to the 'noise subspace' (orthogonal complement of the column span of $\mathbf{A}$). Thus, the submatrix $\widehat{\mathbf{E}}_n$ (containing the last $N - D$ columns of $\widehat{\mathbf{E}}$) is used to either plot a MUSIC spectrum [16]

$$P(\omega) = \left(\mathbf{a}^H(\omega)\widehat{\mathbf{E}}_n\widehat{\mathbf{E}}_n^H\mathbf{a}(\omega)\right)^{-1} \tag{7}$$

or form a root-MUSIC polynomial [26]

$$Q(z) = \mathbf{a}^T(z^{-1})\widehat{\mathbf{E}}_n\widehat{\mathbf{E}}_n^H\mathbf{a}(z), \tag{8}$$

where $\mathbf{a}(z) = \begin{bmatrix} z^{n_1} & z^{n_2} & \dots & z^{n_N} \end{bmatrix}^T$. From the MUSIC spectrum $P(\omega)$, DOAs are estimated from the location of peaks. Root-MUSIC estimates the DOAs from the phases of the D complex-conjugate pairs of roots of $Q(z)$ that are closest to the unit circle. Root-MUSIC is usually applied if the array is ULA (i.e. $n_i = i - 1$). The Cramér-Rao bound (CRB) for DOA estimation and analytical mean squared error expression for MUSIC and root-MUSIC are derived in [27], [28], [29].

A. Effect of Mutual Coupling Between Sensors

When sensors have electromagnetic coupling between them, the array output does not follow the standard model (Eq. (3)). This is called the mutual coupling effect, and it is challenging to precisely model mathematically [22]. In practice, it is usually unknown to the user. In numerical simulations, the effect of coupling is typically modeled as [9], [21], [30]

$$\mathbf{x}[k] = \mathbf{C}\mathbf{A}\mathbf{s}[k] + \mathbf{n}[k], \tag{9}$$

where $\mathbf{C}$ is the coupling matrix with entries $\mathbf{C}_{i,j} = c_{|n_i - n_j|}$, and the coupling coefficients c_l are non-zero for $l \leq B$. Here, $c_0 = 1$, and the rest of the non-zeros coupling coefficients $c_l, 1 \leq l \leq B$ have their magnitudes inversely proportional to l, i.e. $|c_m/c_n| = n/m$. For ULA, $\mathbf{C}$ is a banded Toeplitz matrix. The coupling strength is characterized by $|c_1| = c$. Another metric to characterize the amount of mutual coupling is the coupling leakage defined as

$$\mathcal{L} = \frac{||\mathbf{C} - \mathrm{diag}(\mathbf{C})||_F}{||\mathbf{C}||_F}. \tag{10}$$

where $||\cdot||_F$ denotes the Frobenius norm. To mitigate the impact of mutual coupling on DOA estimation, some papers [31], [32], [33] estimate the coupling matrix along with the DOAs. Another approach is to design sparse arrays in such a way that the effect of mutual coupling on DOA estimation is reduced. This is the motivation for the sparse array design criterion, which aims to reduce the weights $w(1), w(2)$, and $w(3)$ that contribute the most to the mutual coupling effect. In this paper, we do not explicitly account for mutual coupling algorithmically but rather design sparse arrays that can effectively handle the presence of mutual coupling. To the best of our knowledge, a Cramér-Rao bound (CRB) for DOA estimation in the presence of mutual coupling is not known in the literature.

B. A Note on the Practicality of the Mutual Coupling Model

While this basic phenomenon of coupling is a direct consequence of Faraday's law of induction, the actual application in an antenna array is quite complicated (for example, see p. 475 of [34], and [35]). Furthermore, the geometry of the antennas used in the array (i.e., whether they are dipole antennas, sleeve dipole antennas, spiral antennas, etc.) plays a role in determining the mutual coupling behavior [36], [37], [38]. The coupling matrix $\mathbf{C}$ is actually the inverse of a so-called normalized impedance matrix $\mathbf{Z}_0$ that has been used to model the self- and mutual-coupling in the antenna elements [31], [39], [40], [41]. As seen from these references, there are multiple ways to formulate the matrix $\mathbf{Z}_0$, and they yield quite different results. A summary of different methods and their pros and cons can be found in [35]. While these papers are insightful, they do not offer any way to estimate the ratio $c = |c_1|$ which actually comes from the inverse $\mathbf{Z}_0^{-1}$.

The element $[\mathbf{Z}_0]_{k,m}$ is proportional to z_{km} which is the mutual impedance between the kth and mth sensor. These impedances are approximately proportional to $1/(n_k - n_m)$. This is consistent with the fact that the radiation term for the electric field from an accelerated charge (as in the case of a sinusoidal current in an antenna wire) varies as $1/r$ rather than as $1/r^2$ (Chap. 28 of [42]). The $1/r$ assumption has been used in the past, and it can be verified in the estimates of impedances reported in Table 1 of [40] and Table 2 of [41]. The fact that the dependence is not exactly of the form $1/r$ is well known even from basic examples such as can be found on page 189 of [43] (e.g., set $d >> a, b$ in Eqs. (10) and (11) therein).

Now, it is difficult to see how the above assumption on $[\mathbf{Z}_0]_{k,m}$ reflects in the matrix $\mathbf{C}$. As explained earlier, it is often assumed that $\mathbf{C}_{i,j} = c_{|n_i - n_j|}$ and that $|c_m/c_n| = n/m$. While this is similar to the properties of $[\mathbf{Z}_0]_{k,m}$, it is hard to give a theoretical justification that the properties of $\mathbf{Z}_0$ will be inherited like this by the elements of the inverse $\mathbf{C} = \mathbf{Z}_0^{-1}$. A more detailed description of the difficulties involved in modeling mutual coupling can be found in [44]. However, this model of mutual coupling has been widely used [9], [30], [31] in the signal processing community and the same is used in this paper as well.

As mentioned before, the goal of this paper is to design sparse arrays that can effectively handle the presence of mutual coupling without its explicit knowledge. That is, we do not attempt to estimate the coupling matrix $\mathbf{C}$ or compensate for its effect algorithmically. In this paper, we simply apply coarray-based DOA estimation with appropriate modifications, a brief summary of which is provided next.

C. Coarray-Based DOA Estimation

Based on the eigendecomposition of $\widehat{\mathbf{R}}_x$, one can identify only up to $N-1$ DOAs because the size of $\widehat{\mathbf{R}}_x$ is $N \times N$. Instead, array output correlations can be first estimated at each lag l in the difference coarray $\mathbb{D}_{\mathbf{z}}$ as

$$\widehat{R}(l) = \frac{1}{w(l)} \sum_{n_i - n_j = l} [\widehat{\mathbf{R}}_x]_{i,j}. \tag{11}$$

The ideal array output correlations (obtained by using $\mathbf{R}_x$ instead of $\widehat{\mathbf{R}}_x$ in Eq. (11)) have the form

$$R(l) = \sum_{i=1}^{D} p_i e^{j\omega_i l} + \sigma_n^2 \delta(l), \tag{12}$$

where $\delta(l) = 1$ when $l = 0$, and 0 otherwise. DOA estimation performed using the estimated correlations $\widehat{R}(l)$, $l \in \mathbb{D}_{\mathbf{z}} = \{n_i - n_j\}_{i,j=1}^{N}$ is called coarray-based DOA estimation. Note that $\mathbb{D}_{\mathbf{z}}$ can contain up to $N^2 - N + 1$ distinct elements and is symmetric around 0. We use $\mathbb{D}_{\mathbf{z}}^{+}$ to refer to the non-negative part of $\mathbb{D}_{\mathbf{z}}$.

Well-designed sparse arrays contain a large segment of contiguous lags in $\mathbb{D}_{\mathbf{z}}$, which starts at L_1 and ends at L_2 (i.e. $w(l) \neq 0$ for $L_1 \leq l \leq L_2$). Such a segment is called a 'central ULA segment' when $L_1 = -L_2$. For arrays with a central ULA segment in the coarray, a coarray covariance matrix is formed either by spatial smoothing ($\widehat{\mathbf{R}}_{SS}$) [5] or by direct-augmentation approach ($\widehat{\mathbf{R}}_{DA}$) [17]. As shown in [17], $\widehat{\mathbf{R}}_{DA}$ has entries $[\widehat{\mathbf{R}}_{DA}]_{m,n} = \widehat{R}(m-n)$ and $\widehat{\mathbf{R}}_{SS} = \frac{1}{K}\widehat{\mathbf{R}}_{DA}\widehat{\mathbf{R}}_{DA}^{H}$. Both $\widehat{\mathbf{R}}_{DA}$ and $\widehat{\mathbf{R}}_{SS}$ are Hermitian Toeplitz matrices. Furthermore, $\widehat{\mathbf{R}}_{SS}$ is positive semidefinite, but $\widehat{\mathbf{R}}_{DA}$ may not be. It is equivalent to use either one of these matrices for subspace-based DOA estimation when a large number of snapshots are available. With limited snapshots, the direct-augmentation method can yield better performance as shown in [45]. As the central ULA segments can have lengths as large as $\mathcal{O}(N^2)$, the matrices $\widehat{\mathbf{R}}_{DA}$ and $\widehat{\mathbf{R}}_{SS}$ have size $\mathcal{O}(N^2) \times \mathcal{O}(N^2)$, and can thus identify up to $\mathcal{O}(N^2)$ DOAs. The CRB for estimating $D \geq N$ DOAs was derived in [46], [47] and an analytical mean squared error expression for coarray-MUSIC was derived in [47]. Coarray-MUSIC is known to be asymptotically inefficient (i.e., MSE does not approach CRB, even for a large number of snapshots and SNR) [47], [48]. Some alternate algorithms, such as the weighted least squares [49] method, an augmented Toeplitz matrix reconstruction approach [50], and a weighted proxy covariance matrix construction approach [51], have been proposed in the literature to improve the efficiency of coarray-based DOA estimation.

It is important to note that the fundamental assumption in using sparse arrays and coarray-based estimation of more DOAs than the number of sensors, is that the sources are uncorrelated. Such an assumption is difficult to verify practically and it may not hold, especially in the situations where multipath propagation is possible. Developing algorithms and sparse arrays that are robust to the presence of correlations is of practical interest. One of the recent attempts in this direction is the MESA algorithm [52] based on stochastic maximum likelihood formulation. It is shown in [52] that coarray-based methods can be sensitive to source correlations due to the destruction of the Toeplitz covariance structure, and the MESA algorithm can be robust to source correlations, especially when $D < N$. Further research in this direction is required to enhance the practical utility of sparse arrays.

III. Coarray-MUSIC Using One-Sided ULA Segment in Coarray

The new arrays proposed in this paper do not have a *central* ULA segment in the coarray, as they have $w(1) = 0$. These arrays have one-sided ULA segments in the coarray from lag L_1 to L_2 where $0 < L_1 < L_2$. In this section, we describe how to estimate DOAs using such one-sided ULA segment of length $L = L_2 - L_1 + 1$ in the coarray, and show that up to $\lfloor L/2 \rfloor$ DOAs can be identified using the procedure described. This procedure is similar to the direct-augmentation approach (with matrix $\widehat{\mathbf{R}}_{DA}$) described in Sec. II-C. However, there are some subtleties involved as we explain next.

Similar to $\widehat{\mathbf{R}}_{DA}$, based on the estimated correlations $\widehat{R}(l), L_1 \leq l \leq L_2$, we can create a Toeplitz matrix $\widehat{\mathbf{R}}$:

$$\widehat{\mathbf{R}} = \begin{bmatrix} \widehat{R}(L_2 - r_1 + 1) & \dots & \widehat{R}(L_1) \\ \widehat{R}(L_2 - r_1 + 2) & \dots & \widehat{R}(L_1 + 1) \\ \vdots & \ddots & \vdots \\ \widehat{R}(L_2 - 1) & \dots & \widehat{R}(L_1 + r_1 - 2) \\ \widehat{R}(L_2) & \dots & \widehat{R}(L_1 + r_1 - 1) \end{bmatrix} \tag{13}$$

The matrix $\widehat{\mathbf{R}}$ has size $r_1 \times r_2$, where $r_1 = \lfloor L/2 \rfloor + 1$ and $r_2 = \lceil L/2 \rceil$, and its entries are $\widehat{\mathbf{R}}_{m,n} = \widehat{R}(L_2 - r_1 + 1 + m - n)$. The k-th column of $\widehat{\mathbf{R}}$ contains r_1 consecutive correlations starting from $\widehat{R}(L_1 + r_2 - k)$. Note that when $L_1 = -L_2$, $\widehat{\mathbf{R}} = \widehat{\mathbf{R}}_{DA}$. $\widehat{\mathbf{R}}$ is a square matrix when L is odd, whereas $\widehat{\mathbf{R}}$ is a tall matrix when L is even. Even when $\widehat{\mathbf{R}}$ is square, it is not a Hermitian matrix in general, unlike $\widehat{\mathbf{R}}_{DA}$ and $\widehat{\mathbf{R}}_{SS}$. We would like to note that in [48], two variations of coarray-covariance matrix (namely, 'tall' and 'fat' variations) were proposed. Here, $\widehat{\mathbf{R}}$ is formed in a similar way, but using the correlation entries from a one-sided ULA segment in the coarray. Furthermore, unlike that in [48], the size of $\widehat{\mathbf{R}}$ is fixed and does not depend on the number of DOAs D. The dimensions $(\lfloor L/2 \rfloor + 1) \times \lceil L/2 \rceil$ of the matrix $\widehat{\mathbf{R}}$ are chosen such that the number of DOAs we can identify using a subspace-based algorithm is maximized. As explained next, up to $\lfloor L/2 \rfloor$ DOAs can be identified by computing singular value decomposition (SVD) of $\widehat{\mathbf{R}}$.

To see this, first consider an ideal version of the matrix $\widehat{\mathbf{R}}$, with entries $R(l)$ instead of $\widehat{R}(l)$. With a large number of snapshots, the matrix $\widehat{\mathbf{R}}$ converges to the ideal $r_1 \times r_2$ matrix $\mathbf{R}$ with entries

$$[\mathbf{R}]_{m,n} = R(L_2 - r_1 + 1 + m - n) \tag{14}$$

As the ideal correlations $R(l)$ have the sum-of-sinusoids form (Eq. (12)), the last (i.e. r_2-th) column of $\mathbf{R}$ containing entries

$R(L_1)$ to $R(L_1+r_1-1)$ can be written as

$$\mathbf{R}(:,r_2)=\underbrace{\begin{bmatrix}1 & \dots & 1\\ e^{j\omega_1} & \dots & e^{j\omega_D}\\ \vdots & & \vdots\\ e^{j\omega_1(r_1-1)} & \dots & e^{j\omega_D(r_1-1)}\end{bmatrix}}_{\mathbf{A}_c}\begin{bmatrix}p_1e^{j\omega_1L_1}\\ p_2e^{j\omega_2L_1}\\ \vdots\\ p_De^{j\omega_DL_1}\end{bmatrix} \tag{15}$$

Similarly, the k-th column of $\mathbf{R}$ can be expressed as

$$\mathbf{R}(:,k)=\mathbf{A}_c\mathbf{b}_k \tag{16}$$

where $\mathbf{b}_k$ is a D-dimensional vector with m-th entry $[\mathbf{b}_k]_m = p_m e^{j\omega_m(L_1+r_2-k)}$. Collecting such equations for all columns of $\mathbf{R}$ (i.e. for $k=1,\dots,r_2$), we get

$$\mathbf{R}=\mathbf{A}_c\mathbf{P}\mathbf{B}_c^H \tag{17}$$

where $\mathbf{A}_c$ is an $r_1\times D$ matrix with entries $[\mathbf{A}_c]_{m,n}=e^{j\omega_n(m-1)}$, $\mathbf{P}$ is a $D\times D$ diagonal matrix containing source powers $p_1,\dots,p_D$, and $\mathbf{B}_c$ is an $r_2\times D$ matrix with entries $[\mathbf{B}_c]_{m,n}=e^{-j\omega_n(L_1+r_2-m)}$. Since the DOAs $\omega_1,\dots,\omega_D$ are distinct, as long as $r_1\geq D$ and $r_2\geq D$ the Vandermonde matrices $\mathbf{A}_c$ and $\mathbf{B}_c$ have rank D. Thus, using Sylvester's rank inequality for matrices, it can be concluded that matrix $\mathbf{R}$ also has rank D. Now, as $\mathbf{A}_c$ and $\mathbf{R}$ have the same rank D, and any vector $\mathbf{x}$ satisfying $\mathbf{x}^H\mathbf{A}_c=0$ also satisfies $\mathbf{x}^H\mathbf{R}=0$ (from Eq. (17)), it can be concluded that matrices $\mathbf{A}_c$ and $\mathbf{R}$ have the same column spans.

In practice, we only have access to the matrix $\widehat{\mathbf{R}}$. We can estimate the column span of $\mathbf{A}_c$ (and its orthogonal complement) through an SVD of $\widehat{\mathbf{R}}$:

$$\widehat{\mathbf{R}}=\widehat{\mathbf{U}}\widehat{\mathbf{\Sigma}}\widehat{\mathbf{V}}^H, \tag{18}$$

where $\widehat{\mathbf{U}}$ is an $r_1\times r_1$ matrix with orthonormal columns, and $\widehat{\mathbf{\Sigma}}$ is an $r_1\times r_2$ matrix containing singular values arranged in descending order along the principal diagonal. The first D columns of $\widehat{\mathbf{U}}$ provide an approximation to the column span of $\mathbf{A}_c$. The matrix $\widehat{\mathbf{U}}_n$ containing the last r_1-D columns of $\widehat{\mathbf{U}}$ provides an approximation to the 'noise subspace' (the orthogonal complement of $\mathbf{A}_c$). As long as $D<r_1$, we obtain a non-trivial noise subspace with a dimension of at least one. Thus, by using $\widehat{\mathbf{U}}_n$ in place of $\widehat{\mathbf{E}}_n$, and $\mathbf{a}_c(z)$ (where $[\mathbf{a}_c(z)]_i=z^{i-1}$) in place of $\mathbf{a}(z)$ in Eq. (8), we can get a coarray root-MUSIC polynomial, from which the DOAs can be estimated.

In summary, even when $\widehat{\mathbf{R}}$ is not a square matrix, we can apply SVD to estimate signal subspace and noise subspace from $\widehat{\mathbf{R}}$ and use coarray-based root-MUSIC to estimate DOAs using the one-sided ULA segment from the difference coarray. Note that $D<r_1$ and $D\leq r_2$ for the above-described method to work. Thus, to maximize the number of DOAs we can identify using this approach, $\min(r_1-1,r_2)$ should be as large as possible. As we only have the L contiguous correlation estimates $\widehat{R}(L_1),\dots,\widehat{R}(L_2)$ to form the Teoplitz matrix $\widehat{\mathbf{R}}$, r_1 and r_2 should also satisfy $r_1+r_2-1=L$. Under this constraint, it can be verified that the largest value for $\min(r_1-1,r_2)$ is obtained when $r_1=\lfloor L/2\rfloor+1$ and $r_2=\lceil L/2\rceil$. Thus it is possible to identify a maximum of $r_1-1=\lfloor L/2\rfloor$ DOAs in this way by applying SVD to the matrix $\widehat{\mathbf{R}}$ of size $(\lfloor L/2\rfloor+1)\times\lceil L/2\rceil$.

We would like to note that some previous papers such as [7], [14] have reported DOA estimation performance using a subspace-based algorithm with CADiS arrays that have one-sided ULA segment in coarray. However, they do not describe or justify their method for identifying DOAs using such one-sided ULA segment in coarray, or derive the maximum number of identifiable sources. In fact, the number of identifiable sources reported in [14] for CADiS array when using subspace-based DOA estimation is one less than $\lfloor L/2\rfloor$ when L is even.

It is possible to use techniques other than coarray-based algorithms to identify more DOAs than the number of sensors. Some examples include the weighted least squares method [49], stochastic maximum likelihood estimation [52], and dictionary-based methods [53]. This paper primarily focuses on introducing new sparse arrays that can handle strong mutual coupling and aperture constraints, rather than focusing on various algorithms that can be applied for DOA estimation. With suitable adaptations, it is possible to use other DOA estimation algorithms with the proposed arrays. This section demonstrated the adaptation of widely used coarray-MUSIC for one-sided ULA segments in the difference coarray.

IV. Proposed Weight-Constrained Sparse Arrays With $\mathcal{O}(N)$ Aperture

In this section, we first systematically develop sparse arrays that have an aperture of $\mathcal{O}(N)$ length and $w(1)=0$. We will start by explaining a procedure to generate such arrays by properly dilating a ULA and adding a few extra sensors. We will then propose modifications to the construction to make other crucial weights ($w(2)$ and $w(3)$) small constants independent of N while keeping $w(1)=0$. We will also develop sparse arrays that have $\mathcal{O}(N)$ aperture and $w(1)=w(2)=0$. Moreover, we will discuss further modifications to make $w(3)$ and $w(4)$ small constants independent of N. The coarray properties of the arrays proposed in this section are summarized in Table II. These arrays will be called 'weight-constrained sparse arrays'. We assume $N>5$ to ensure that the general expressions for all arrays are valid.

A. Proposed Sparse Arrays With $\mathcal{O}(N)$ Aperture and $w(1)=0$

We want to create a sparse array with $\mathcal{O}(N)$ aperture and $w(1)=0$. We also want to ensure that the array has a large ULA segment in its coarray from lag two onwards for easy application of coarray root-MUSIC. To achieve this we follow these steps:

1) Expand an $(N-1)$-sensor ULA by a factor of two to create a '2-sparse' ULA $\{0,2,...,2(N-2)\}$. This is called the array *dilation* step.
2) Place the N-th sensor at location $2N-1$. This is called the array *augmentation* step.

Thus, we get the array:

$$\mathbf{z}_1=\big[\underbrace{0\quad 2\quad 4\quad \dots\quad 2(N-2)}_{\text{2-sparse ULA}}\quad 2N-1\big] \tag{19}$$

TABLE II
COARRAY PROPERTIES OF THE WEIGHT-CONSTRAINED SPARSE ARRAYS WITH $\mathcal{O}(N)$ APERTURE PROPOSED IN SEC.IV. ARRAY APERTURE (A), COARRAY WEIGHTS $w(l)$, ULA SEGMENT IN THE COARRAY, COARRAY HOLES, AND MAXIMUM NUMBER OF IDENTIFIABLE DOAS WITH COARRAY-MUSIC D_m ARE COMPARED. 'A' IN THE SECOND LAST COLUMN REFERS TO THE APERTURE LISTED IN THE SECOND COLUMN. ARRAY $\mathbf{z}_6$ HAS $w(1) = w(2) = 0$ AND CONSTANT $w(3)$ AND $w(4)$ INDEPENDENT OF N

Array	Aperture A	Coarray Weights $w(1)$	$w(2)$	$w(3)$	$w(4)$	$w(5)$	ULA Segment in Coarray Start (L_1)	End (L_2)	Length (L)	Holes in Coarray	D_m
ULA	$N-1$	$N-1$	$N-2$	$N-3$	$N-4$	$N-5$	$-N+1$	$N-1$	$2N-1$	None	$N-1$
$\mathbf{z}_1$	$2N-1$	0	$N-2$	1	$N-3$	1	2	$2N-3$	$2N-4$	$1, A-1$	$N-2$
$\mathbf{z}_2^{(1)}$	$3N-5$	0	2	$N-3$	1	1	2	$3N-7$	$3N-8$	$1, A-1$	$\lfloor 1.5N \rfloor - 4$
$\mathbf{z}_2^{(2)}$	$3N-3$	0	1	$N-3$	1	1	2	$3N-7$	$3N-8$	$1, A-3, A-1$	$\lfloor 1.5N \rfloor - 4$
$\mathbf{z}_3^{(1)}$	$4N-9$	0	2	1	$N-4$	1	2	$4N-13$	$4N-14$	$1, A-3, A-1$	$2N-7$
$\mathbf{z}_3^{(2)}$	$4N-8$	0	1	2	$N-4$	1	2	$4N-13$	$4N-14$	$1, A-4, A-2, A-1$	$2N-7$
$\mathbf{z}_4$	$3N$	0	0	$N-3$	1	1	3	$3N-7$	$3N-9$	$1, 2, A-6, A-3, A-2, A-1$	$\lfloor (3N-9)/2 \rfloor$
$\mathbf{z}_5$	$4N-5$	0	0	2	$N-4$	1	3	$4N-13$	$4N-15$	$1, 2, A-7, A-4 A-2, A-1$	$2N-8$
$\mathbf{z}_6$	$5N-12$	0	0	3	1	$N-5$	3	$5N-21$	$5N-23$	$1, 2, A-8, A-5, A-4, A-2, A-1$	$\lfloor (5N-23)/2 \rfloor$

Note that the coarray of the 2-sparse ULA consists only of the even lags from $-2(N-2)$ to $2(N-2)$. The augmented sensor is placed at a distance three from the last sensor of the 2-sparse ULA and is at odd distances from the other $N-1$ sensors. This creates lags $3, 5, \ldots, 2N-1$ in the coarray, which were missing from the coarray of the 2-sparse ULA. Thus, the coarray $\mathbb{D}^+_{\mathbf{z}_1}$ of $\mathbf{z}_1$ is

$$\mathbb{D}^+_{\mathbf{z}_1} = \{0, \underbrace{2, 3, 4, \ldots, 2N-4, 2N-3}_{\text{One-sided ULA segment in coarray}}, 2N-1\} \tag{20}$$

The array $\mathbf{z}_1$ has an aperture $A = 2N-1$ and its coarray includes a ULA segment of length $L = 2N-4$ starting from $L_1 = 2$ and ending at $L_2 = 2N-3$. Since the coarray is symmetric, it also contains a ULA segment from $-L_2$ to $-L_1$. As explained in Sec. III, we can identify up to $\lfloor L/2 \rfloor = N-2$ DOAs by using coarray root-MUSIC with this array. Although an N-sensor ULA can identify one more DOA than $\mathbf{z}_1$, the proposed array can tolerate mutual coupling better than the ULA, as we will see in Section VI, because it has $w(1) = 0$.

Note that the coarray $\mathbb{D}^+_{\mathbf{z}_1}$ has two holes located at positions 1 and $2N-2$. It is not possible to eliminate the extra hole at position $2N-2$. For any array that has $w(1) = 0$, $w(A-1)$ must also be zero. This is because there are sensors at 0 and A for an array with aperture A. No sensor can be placed at either location 1 or $A-1$, as that will create a sensor pair with separation 1. With no sensors at 1 and $A-1$, $w(A-1)$ must be zero. Thus, there are no holes in the coarray $\mathbb{D}^+_{\mathbf{z}_1}$ apart from those that arise as a necessary consequence of our design constraint $w(1) = 0$.

B. Further Reducing $w(2)$ and $w(3)$

Even though the array $\mathbf{z}_1$ can make $w(1)$ equal to zero, it has $w(2)$ equal to $N-2$ because of the 2-sparse ULA segment in the array. To further reduce the mutual coupling, we need to construct an array where $w(2)$ is a small constant independent of the number of sensors, while also ensuring that $w(1)$ is zero. To achieve this, we can start with a '3-sparse' ULA having $(N-2)$ sensors and add two more sensors at a distance of either 2 or 4 units from the same end or opposite ends of the 3-sparse ULA.

Augmenting both sensors on the same side gives the array:

$$\mathbf{z}_2^{(1)} = \big[\underbrace{0 \quad 3 \quad 6 \quad \ldots \quad 3(N-3)}_{\text{3-sparse ULA}} \quad 3N-7 \quad 3N-5\big], \tag{21}$$

and its coarray is $\mathbb{D}^+_{\mathbf{z}_2^{(1)}} = \{0, 2, 3, \ldots, 3N-8, 3N-7, 3N-5\}$. The ULA segment in the coarray (underlined) is from $L_1 = 2$ to $L_2 = 3N-7$. Similar to the previous design, the coarray has only two holes located at positions 1 and $3N-6$ $(= A-1)$. An important advantage of this design over $\mathbf{z}_1$ is that $w(2) = 2$, independent of the number of sensors N used. This further reduces the impact of mutual coupling compared to the previous design $\mathbf{z}_1$. However, $\mathbf{z}_2^{(1)}$ has larger aperture than $\mathbf{z}_1$.

Instead of placing both additional sensors on the same side, they can be placed on opposite sides of the 3-sparse ULA:

$$\mathbf{z}_2^{(2)} = \big[-2 \quad \underbrace{0 \quad 3 \quad 6 \quad \ldots \quad 3(N-3)}_{\text{3-sparse ULA}} \quad 3N-5\big]. \tag{22}$$

By doing so, $w(2)$ now becomes 1 instead of 2. The coarray still has ULA segment from 2 to $3N-7$, but the array aperture is now $3N-3$ instead of $3N-5$, and the coarray $\mathbb{D}^+_{\mathbf{z}_2^{(2)}}$ has three holes at 1, $3N-6$ $(= A-3)$, and $3N-4$ $(= A-1)$.

The arrays $\mathbf{z}_2^{(1)}$ and $\mathbf{z}_2^{(2)}$ make $w(2)$ a constant independent of the number of sensors N, but their $w(3)$ increases linearly with N because of the 3-sparse ULA segment in the array. To make $w(1) = 0$ and both $w(2)$ and $w(3)$ small constants, we propose the following construction. We use a 4-sparse ULA of $N-3$ sensors with appropriately placed three other sensors:

$$\mathbf{z}_3^{(1)} = \big[-2 \quad \underbrace{0 \quad 4 \quad \ldots \quad 4(N-4)}_{\text{4-sparse ULA}} \quad 4N-13 \quad 4N-11\big]. \tag{23}$$

TABLE III
COARRAY PROPERTIES OF THE PROPOSED WEIGHT-CONSTRAINED NESTED ARRAYS WITH $\mathcal{O}(N^2)$ APERTURE PROPOSED IN SEC.V. FOR A GIVEN NUMBER OF SENSORS N, THE OPTIMAL VALUES OF N_1 AND N_2 FOR NESTED ARRAY ARE $N_1 = \text{round}((N+1)/2)$, AND $N_2 = N - \text{round}((N+1)/2)$ [5]. WE ASSUME $N_1 \geq 5$. THE OPTIMAL VALUES OF N_1 AND N_2 FOR $\mathbf{w}_1^{(1)}$ AND $\mathbf{w}_1^{(2)}$ ARE GIVEN BY EQ. (29), AND THAT FOR $\mathbf{w}_2$ ARE GIVEN BY EQ. (34). THE MAXIMUM NUMBER OF IDENTIFIABLE DOAS WITH COARRAY-MUSIC IS $\lfloor L/2 \rfloor$

Array	Aperture	Coarray Weights					ULA Segment in Coarray		
	A	$w(1)$	$w(2)$	$w(3)$	$w(4)$	$w(5)$	Start (L_1)	End (L_2)	Length (L)
Nested	$(N_1+1)N_2-1$	N_1	N_1-1	N_1-2	N_1-3	N_1-4	-A	A	$2(N_1+1)N_2-1$
$\mathbf{w}_1^{(1)}$	$2(N_1+1)N_2+1$	0	N_1	N_2	N_1-1	1	2	$2(N_1+1)N_2-1$	$2(N_1+1)N_2-2$
$\mathbf{w}_1^{(2)}$	$2(N_1+1)(2N_2-1)+1$	0	N_1	1	N_1-1	1	2	$2(N_1+1)N_2-1$	$2(N_1+1)N_2-2$
$\mathbf{w}_2$	$3(N_1+1)(2N_2-1)+6$	0	0	N_1	1	N_2	3	$3(N_1+1)N_2-1$	$3(N_1+1)N_2-3$

Its coarray is $\mathbb{D}_{\mathbf{z}_3}^{+} = \{0, 2, 3, 4, \ldots, 4N-14, 4N-13, 4N-11, 4N-9\}$. This array construction has constant $w(1) = 0$, $w(2) = 2$, $w(3) = 1$ independent of the number of sensors N, and its coarray has ULA segment from $L_1 = 2$ to $L_2 = 4N-13$. By rearranging the three additionally placed sensors, we get another variation of this array configuration

$$\mathbf{z}_3^{(2)} = \big[-5 \quad -2 \quad \underbrace{0 \quad 4 \quad \ldots \quad 4(N-4)}_{\text{4-sparse ULA}} \quad 4N-13\big]. \quad (24)$$

The advantage of this array over $\mathbf{z}_3^{(1)}$ is that $w(2)$ is reduced to 1. In the next subsection, to further reduce the impact of mutual coupling, we develop sparse arrays with $w(1) = w(2) = 0$.

C. Proposed Arrays With $\mathcal{O}(N)$ Aperture and $w(1) = w(2) = 0$

We can construct $\mathcal{O}(N)$ aperture arrays that have both $w(1) = w(2) = 0$ by using a similar construction mechanism of ULA dilation and augmentation. Consider an array with 3-sparse ULA of $N-2$ sensors and two additional sensors placed at distances of 4 and 5 units from the opposite ends of the 3-sparse ULA:

$$\mathbf{z}_4 = \big[-5 \quad \underbrace{0 \quad 3 \quad 6 \quad \ldots \quad 3(N-3)}_{\text{3-sparse ULA}} \quad 3N-5\big]. \quad (25)$$

The sensor located at $3N-5$ is positioned at a distance of 4 from one end of the 3-sparse ULA. This sensor produces differences $\{4, 7, 10, \ldots, 3N-5\}$ with the sensors of the 3-sparse ULA. On the other hand, the sensor at -5 is located at a distance of 5 from the opposite end of the 3-sparse ULA and creates differences $\{5, 8, 11, \ldots, 3N-4\}$ with the sensors of the 3-sparse ULA. When combined with the self-differences $\{0, 3, 6, \ldots, 3(N-3)\}$ created by the sensor pairs within 3-sparse ULA, we get that the coarray of $\mathbf{z}_4$ is $\mathbb{D}_{\mathbf{z}_4}^{+} = \{0, 3, 4, 5 \ldots, 3(N-3), 3N-8, 3N-7, 3N-5, 3N-4, 3N\}$. The largest difference of $3N$ is between the two augmented sensors.

This array with an aperture of length $3N$ has $w(1) = w(2) = 0$. Its coarray contains a ULA segment starting from $L_1 = 3$ and ending at $L_2 = 3N-7$. It can identify up to $\lfloor (3N-9)/2 \rfloor$ DOAs using coarray root-MUSIC. In addition to the holes at 1, and 2, the coarray has four additional holes located at $3N-6$, $3N-3$, $3N-2$, and $3N-1$.

D. Further Reducing $w(3)$ and $w(4)$

Although $\mathbf{z}_4$ has $w(1) = w(2) = 0$, its $w(3)$ increases as N increases. To make $w(3)$ constant we consider the following array:

$$\mathbf{z}_5 = \big[-5 \quad \underbrace{0 \quad 4 \quad 8 \quad \ldots \quad 4(N-4)}_{\text{4-sparse ULA}} \quad 4N-13 \quad 4N-10\big]. \quad (26)$$

Array $\mathbf{z}_5$ consists of a 4-sparse ULA of $N-3$ sensors and three additional sensors placed at positions -5, $4N-13$, and $4N-10$. The 4-sparse ULA creates self-differences $4\,[[0, N-4]]$ in the coarray. The sensor at location -5 is at a distance 5 from the 4-sparse ULA segment, and creates differences $4\,[[1, N-3]] + 1$. The sensor at location $4N-13$ is at distance 3 from the 4-sparse ULA segment, and creates differences $4\,[[1, N-3]] - 1$. The sensor at location $4N-10$ is at distance 6 from the 4-sparse ULA segment, and creates differences $4\,[[1, N-3]] + 2$. Combined with the additional differences $4N-8$ and $4N-5$ between the augmented sensors, we get that the coarray of $\mathbf{z}_5$ is $\mathbb{D}_{\mathbf{z}_5}^{+} = \{0, 3, 4, 5, \ldots, 4N-13, 4N-11, 4N-10, 4N-8, 4N-5\}$. The ULA segment in the coarray is from $L_1 = 3$ to $L_2 = 4N-13$. The coarray has four holes in addition to the holes at positions 1 and 2.

The first three weights $w(l), 1 \leq l \leq 3$ of $\mathbf{z}_5$ do not increase with N. We can go a step further to also make $w(4)$ a constant by considering the following array:

$$\mathbf{z}_6 = \big[-7 \quad -4 \quad \underbrace{0 \quad 5 \quad \ldots \quad 5(N-5)}_{\text{5-sparse ULA}} \quad 5N-22 \quad 5N-19\big]. \quad (27)$$

Array $\mathbf{z}_6$ consists of a 5-sparse ULA of $N-4$ sensors and four augmented sensors placed at positions -7, -4, $5N-22$, and $5N-19$. The 5-sparse ULA creates self-differences $5\,[[0, N-5]]$. The sensor at location $5N-19$ creates differences $5\,[[1, N-4]] + 1$, the sensor at location -7 creates differences $5\,[[1, N-4]] + 2$, the sensor at location $5N-22$ creates differences $5\,[[1, N-4]] - 2$, and the sensor at location -4 creates differences $5\,[[1, N-4]] - 1$ with the sensors from the 5-sparse ULA segment. Combined with the additional differences $5N-12$ and $5N-15$ between the augmented sensors, we get that the coarray of $\mathbf{z}_6$ is $\mathbb{D}_{\mathbf{z}_6}^{+} = \{0, 3, 4, 5 \ldots, 5N-21, 5N-19, 5N-18, 5N-15, 5N-12\}$. The ULA segment in the coarray (underlined) is from $L_1 = 3$ to $L_2 = 5N-21$. The array has $w(1) = w(2) = 0$,

$w(3) = 3$, and $w(4) = w(6) = w(7) = w(8) = w(9) = 1$, and $w(5) = N - 5$. Out of the first nine coarray weights $w(l), 1 \leq l \leq 9$, only $w(5)$ increases with the number of sensors N. There are five holes in addition to the holes at positions 1 and 2 in the coarray.

V. Proposed Weight-Constrained Nested Arrays With $\mathcal{O}(N^2)$ Aperture

In this section, we develop sparse arrays with $\mathcal{O}(N^2)$ aperture that have either $w(1) = 0$ or $w(1) = w(2) = 0$. For arrays in the previous section, we expanded a ULA and added a few extra sensors. For $\mathcal{O}(N^2)$ aperture arrays, we will start by expanding a nested array. However, we will need to add several extra sensors to ensure that the coarray has a ULA segment from lag 2 or 3 onwards. These arrays will be called 'weight-constrained nested arrays'. These arrays are well-suited for identifying a large number of DOAs under high mutual coupling, as we will see in Sec. VI. However, they have large apertures, and so they are not suitable when there is an aperture constraint. Coarray properties of the arrays described in this section are summarized in Table III.

A. Weight-Constrained Nested Arrays With $w(1) = 0$

Consider a standard nested array [5] $\mathbf{z}_n = \mathbb{P}_1 \cup \mathbb{P}_2$ where, $\mathbb{P}_1 = [[1, N_1]]$ and $\mathbb{P}_2 = (N_1 + 1)\,[[1, N_2]]$. We assume that $N_1 > 3$, so that the general expressions are valid. The coarray of the nested array is $\mathbb{D}^+_{\mathbf{z}_n} = [[0, (N_1 + 1)N_2 - 1]]$. Now consider the array

$$\mathbf{w}_1^{(1)} = (2\mathbb{P}_1) \cup (2\mathbb{P}_2) \cup \mathbb{P}_3, \tag{28}$$

where $\mathbb{P}_3 = 2\mathbb{P}_2 + 3$. This array $\mathbf{w}_1^{(1)}$ is formed by first expanding a nested array to create a '2-sparse' nested array $(2\mathbb{P}_1) \cup (2\mathbb{P}_2)$ and appending it with another sparse ULA segment $\mathbb{P}_3$ containing N_2 sensors. $\mathbb{P}_3$ is just a shifted version of $2\mathbb{P}_2$ to the right by three units. Note that the coarray of the dilated nested array $(2\mathbb{P}_1) \cup (2\mathbb{P}_2)$ only contains even lags from $-2(N_1 + 1)N_2 + 2$ to $2(N_1 + 1)N_2 - 2$. Thus, we append $\mathbb{P}_3$ to fill up the missing odd lags (except the lag 1, to ensure $w(1) = 0$). The array has a total of $N_1 + 2N_2$ sensors and its aperture $A = 2(N_1 + 1)N_2 + 1$ is slightly larger than twice that of the original nested array $\mathbf{z}_n$. We will now prove that the coarray of $\mathbf{w}_1^{(1)}$ has a ULA segment from $L_1 = 2$ to $L_2 = 2(N_1 + 1)N_2 - 1$.

Lemma 1: The difference coarray $\mathbb{D}^+_{\mathbf{w}_1^{(1)}}$ of $\mathbf{w}_1^{(1)}$ contains a ULA segment from $L_1 = 2$ to $L_2 = 2(N_1 + 1)N_2 - 1$.

Proof: As the difference coarray of the nested array is $\mathbb{D}^+_{\mathbf{z}_n} = [[0, (N_1 + 1)N_2 - 1]]$, it is easy to see that all even differences from 0 to $2(N_1 + 1)N_2 - 2$ are created by the sensors from $(2\mathbb{P}_1) \cup (2\mathbb{P}_2)$. Now consider the first sensor from $\mathbb{P}_3$ located at $2(N_1 + 1) + 3$. It creates odd differences $\{3, 5, \ldots, 2(N_1 + 1) + 1\} = 2\,[[1, (N_1 + 1)]] + 1$ with the sensors from $2\mathbb{P}_1 \cup \{2(N_1 + 1)\}$. Similarly, the k-th sensor in $\mathbb{P}_3$ located at $2(N_1 + 1)k + 3$ creates differences of the form $2\,[[1, (N_1 + 1)]] + 2(N_1 + 1)(k - 1) + 1$ with the sensor from $2\mathbb{P}_1 \cup \{2(N_1 + 1)\}$. Putting together these differences for all sensors in $\mathbb{P}_3$ (i.e., for $k \in [[1, N_2]]$), we get that $\mathbb{P}_3$ generates all odd differences from $2\,[[1, (N_1 + 1)N_2]] + 1$. Furthermore, when $N_1 > 1$, there are no sensor pairs with unit separation, and thus $w(1) = w(A - 1) = 0$. Thus, we have proved that the difference coarray of $\mathbf{w}_1^{(1)}$ is $\mathbb{D}^+_{\mathbf{w}_1^{(1)}} = \{0, \underline{2, 3, 4, \ldots, 2(N_1 + 1)N_2 - 1}, 2(N_1 + 1)N_2 + 1\}$ which contains a ULA segment from $L_1 = 2$ to $L_2 = 2(N_1 + 1)N_2 - 1$. □

The array has $w(1) = 0$, and the difference coarray $\mathbb{D}_{\mathbf{w}_1^{(1)}}$ has only two holes, one at location 1 and the other at location $A - 1$. The length of the ULA segment in the coarray is $L = L_2 - L_1 + 1 = 2(N_1 + 1)N_2 - 2$, and thus the number of identifiable DOAs is $\lfloor L/2 \rfloor = (N_1 + 1)N_2 - 1$, which is same as the number of identifiable DOAs with the original nested array $\mathbf{z}_n$. However $\mathbf{w}_1^{(1)}$ uses N_2 additional sensors compared to $\mathbf{z}_n$. Furthermore, when $N_1 > 3$, it can be verified that $w(2) = N_1$, $w(3) = N_2$, $w(4) = N_1 - 1$, and $w(5) = 1$.

For a total number of sensors N, optimal N_1 and N_2 to maximize the ULA segment in the coarray of $\mathbf{w}_1^{(1)}$ are found by solving

$$\begin{aligned} \max_{N_1, N_2} \quad & 2(N_1 + 1)N_2 - 2 \\ \text{s.t.} \quad & N_1 + 2N_2 = N \end{aligned} \tag{29}$$

The optimal solution to the above problem is given by $N_2 = \text{round}((N + 1)/4)$, and $N_1 = N - 2N_2$. With the optimal values of N_1 and N_2, the maximum number of identifiable DOAs is $\mathcal{O}(N^2)$ (approximately $(N + 1)^2/8 - 2$). Thus, the array $\mathbf{w}_1^{(1)}$ can identify $\mathcal{O}(N^2)$ DOAs using coarray-MUSIC.

TABLE IV
Properties of Arrays With $N = 16$. The Last 9 Arrays ($\mathbf{z}_1$ to $\mathbf{w}_2$) Are the New Proposed Arrays. Coupling Leakage $\mathcal{L}$ Is Calculated With $c = 0.3$ and $B = 10$. MSE for Estimating 22 DOAs Is the Smallest for Arrays With $w(1) = 0$ (see Sec. VI-A)

Array	A	$\mathcal{L}$	D_m	Coarray Weights					MSE
				w(1)	w(2)	w(3)	w(4)	w(5)	
SNA2	71	0.2139	71	2	5	4	1	6	0.0174
ANAII-2	84	0.2071	84	2	5	2	3	4	0.0285
EGCA	88	0.1447	65	1	6	1	4	1	0.0772
DNA	77	0.1843	71	1	6	1	4	1	0.0716
DDNA	86	0.1738	72	1	5	1	3	1	0.0748
MISC	83	0.1865	83	1	6	1	4	2	0.093
MRA	90	0.2299	90	4	2	1	1	3	0.0315
cMRA	80	0.1489	38	0	5	2	4	3	0.0001
CPA	63	0.1997	39	2	2	2	9	2	0.0172
CADiS	88	0.1113	30	0	0	7	0	0	0.0001
TCA	75	0.1515	47	1	1	1	2	10	0.0658
ePCA	85	0.1623	65	1	2	1	8	1	0.0369
ULA	15	0.4443	15	15	14	13	12	11	-
$\mathbf{z}_1$	31	0.233	14	0	14	1	13	1	-
$\mathbf{z}_2^{(2)}$	45	0.1592	20	0	1	13	1	1	-
$\mathbf{z}_3^{(2)}$	56	0.1290	25	0	1	2	12	1	0.0002
$\mathbf{z}_4$	48	0.1506	19	0	0	13	1	1	-
$\mathbf{z}_5$	59	0.118	24	0	0	2	12	1	0.0005
$\mathbf{z}_6$	68	0.1061	28	0	0	3	1	11	0.0003
$\mathbf{w}_1^{(1)}$	73	0.1875	35	0	8	4	7	1	0.0003
$\mathbf{w}_1^{(2)}$	127	0.1779	35	0	8	1	7	1	0.0001
$\mathbf{w}_2$	126	0.117	34	0	0	7	1	3	0.0002

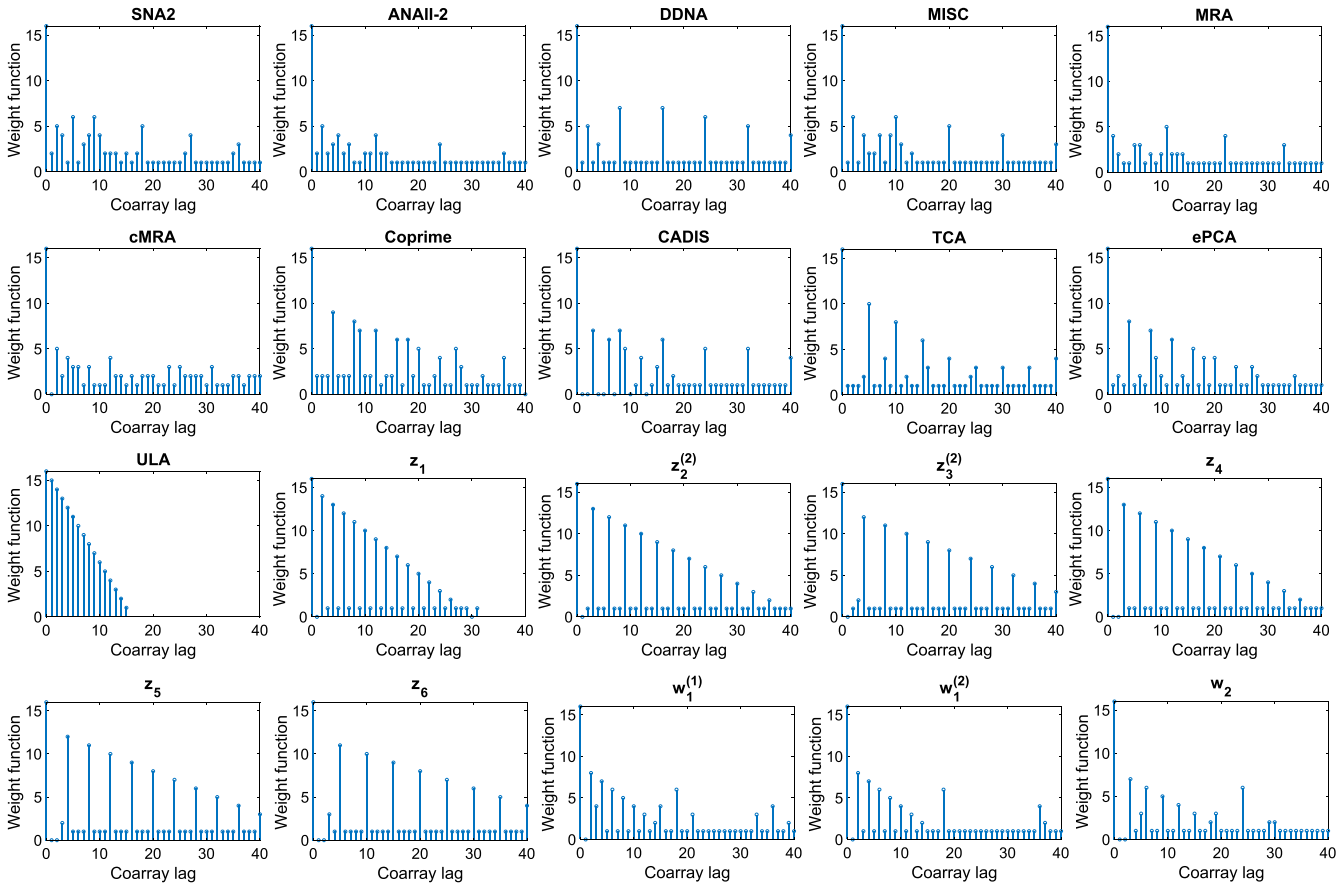

Fig. 1. Coarray weights $w(l), 0 \le l \le 40$ for the arrays under consideration. All arrays have $N = 16$. Out of the proposed arrays shown here, $\mathbf{z}_1$, $\mathbf{z}_2^{(2)}$, $\mathbf{z}_3^{(2)}$, $\mathbf{w}_1^{(1)}$, and $\mathbf{w}_1^{(2)}$ have $w(1) = 0$, and $\mathbf{z}_4$, $\mathbf{z}_5$, $\mathbf{z}_6$, and $\mathbf{w}_2$ have $w(1) = w(2) = 0$. The only other arrays that have $w(1) = 0$ are CADiS [7] and (approximate) constrained MRAs (cMRA) [3]. See Sec. VI-A for details.

Note that $\mathbb{P}_3$ is a $2(N_1+1)$-sparse ULA of N_2 sensors placed at a distance three to the right of the sensors at location $2(N_1+1)$. It was introduced to fill up the odd-valued differences missing from the coarray of the expanded nested array. These odd valued differences are created between the sensors from $\mathbb{P}_3$ and the sensors from the (N_1+1)-sensor 2-sparse ULA segment given by $2\mathbb{P}_1 \cup \{2(N_1+1)\}$. Noting this, we can consider the following variation of the array

$$\mathbf{w}_1^{(2)} = (2\mathbb{P}_1) \cup (2\mathbb{P}_2) \cup \mathbb{P}_3', \tag{30}$$

where $\mathbb{P}_3' = 2\mathbb{P}_2 - 2N_2(N_1+1) - 1$. Here, the $2(N_1+1)$-sparse ULA segment of N_2 sensors $\mathbb{P}_3'$ is placed three units to the left of the sensor at location 2, instead of placing it three units to the right of the sensor at $2(N_1+1)$. Thus, it creates the same set of odd-valued differences with the 2-sparse ULA segment $2\mathbb{P}_1 \cup \{2(N_1+1)\}$. Hence, it can be shown similar to Lemma 1 that array $\mathbf{w}_1^{(2)}$ also has the same ULA segment in its coarray from $L_1 = 2$ to $L_2 = 2(N_1+1)N_2 - 1$. However, the aperture of $\mathbf{w}_1^{(2)}$ is roughly twice that of $\mathbf{w}_1^{(1)}$, and its coarray has many holes, unlike that of $\mathbf{w}_1^{(1)}$ which had only two holes. By shifting the $\mathbb{P}_3$ to the other side of the nested array, $w(3)$ reduces from N_2 to 1. Thus, array $\mathbf{w}_1^{(2)}$ has reduced mutual coupling, at the cost of a larger aperture compared to $\mathbf{w}_1^{(1)}$.

B. Weight-Constrained Nested Arrays With $w(1) = w(2) = 0$

To create a sparse array with $\mathcal{O}(N^2)$ degrees of freedom and $w(1) = w(2) = 0$, we expand a nested array by a factor of 3 and augment it with two additional appropriately placed sparse ULA segments. Consider the array

$$\mathbf{w}_2 = (3\mathbb{P}_1) \cup (3\mathbb{P}_2) \cup \mathbb{P}_4 \cup \mathbb{P}_5 \tag{31}$$

where $\mathbb{P}_1 = [[1, N_1]]$ and $\mathbb{P}_2 = (N_1+1)\,[[1, N_2]]$, and

$$\mathbb{P}_4 = 3\mathbb{P}_2 - 3N_2(N_1+1) - 1 \tag{32}$$

$$\mathbb{P}_5 = 3\mathbb{P}_2 + 5 \tag{33}$$

Here $\mathbb{P}_4$ and $\mathbb{P}_5$ are $3(N_1+1)$-sparse ULA segments of N_2 sensors placed at distances of 4 and 5 units, respectively, from the opposite ends of the 3-sparse ULA segment $3\mathbb{P}_1 \cup \{3(N_1+1)N_2\}$. Array $\mathbf{w}_2$ has a total of $N_1 + 3N_2$ sensors, and its aperture $A = 3(N_1+1)(2N_2-1) + 6$, which is roughly six times that of the original nested array $\mathbf{z}_n$. Similar to Lemma 1, it can be shown that $\mathbf{w}_2$ has a ULA segment in its coarray from $L_1 = 3$ to $L_2 = 3(N_1+1)N_2 - 1$.

Lemma 2: The difference coarray $\mathbb{D}^{+}_{\mathbf{w}_2}$ of $\mathbf{w}_2$ contains a ULA segment from $L_1 = 3$ to $L_2 = 3(N_1+1)N_2 - 1$.

The proof is similar to that of Lemma 1, and details are omitted due to space constraints. The main idea is that the dilated nested array $(3\mathbb{P}_1) \cup (3\mathbb{P}_2)$ creates self-differences $3\,[[0, (N_1+1)N_2 - 1]]$. The sensors from $\mathbb{P}_4$ create differences $3\,[[1, (N_1+1)N_2 - 1]] + 1$ with the sensors from $3\mathbb{P}_1 \cup \{3(N_1+1)N_2\}$. The sensors from $\mathbb{P}_5$ create differences $3\,[[1, (N_1+1)N_2 - 1]] + 2$ with the sensors from $3\mathbb{P}_1 \cup \{3(N_1+1)N_2\}$. Combining the three sets of differences, a ULA segment from $L_1 = 3$ to $L_2 = 3(N_1+1)N_2 - 1$ is obtained.

Array $\mathbf{w}_2$ has $w(1) = w(2) = 0$. However, it has a large aperture and contains several holes in its difference coarray. The length of the one-sided ULA segment in its coarray is $L = 3(N_1+1)N_2 - 3$, and thus it can identify up to $\lfloor L/2 \rfloor \approx 1.5(N_1+1)N_2 - 2$ DOAs with coarray-MUSIC. However $\mathbf{w}_2$ uses $2N_2$ additional sensors compared to $\mathbf{z}_n$. It can be verified that when $N_1 > 3$, $w(3) = N_1$, $w(4) = 1$, and $w(5) = N_2$.

Given N sensors, the optimal N_1 and N_2 to maximize the ULA segment in the coarray of $\mathbf{w}_2$ are found by solving

$$\begin{aligned} \max_{N_1, N_2} \quad & 3(N_1+1)N_2 - 3 \\ \text{s.t.} \quad & N_1 + 3N_2 = N \end{aligned} \tag{34}$$

The optimal solution to the above problem is given by $N_2 = \text{round}((N+1)/6)$, and $N_1 = N - 3N_2$. With the optimal values of N_1 and N_2, the maximum number of identifiable DOAs is $\mathcal{O}(N^2)$ (approximately $(N+1)^2/8 - 2$). Thus, the array $\mathbf{w}_2$ has $w(1) = w(2) = 0$ and can identify $\mathcal{O}(N^2)$ DOAs using coarray-MUSIC.

VI. Simulation Results

In this section, we compare our proposed weight-constrained arrays (with $\mathcal{O}(N)$ aperture array from Sec. IV as well as $\mathcal{O}(N^2)$ aperture arrays from Sec. V) with other sparse arrays from the literature. Out of several generalizations of nested arrays [5], we choose the following four in our comparisons. Super nested arrays (SNA) [9], [10] have the same length of difference coarray as the parent nested arrays, but are more robust to mutual coupling because of reduced coarray weights at small lags. Therefore, we use SNA for comparison instead of nested arrays. We use a third-order super nested array (SNA3) if available, and if not, a second-order super nested array (SNA2) is used. Augmented nested arrays (ANA) [11] are formed by rearranging and distributing the sensors from the dense subarray of the nested array on the two sides of the sparse subarray of the nested array. Out of the four variations of ANAs, we use ANAII-2, which has the largest DOFs and small mutual coupling compared to other variations. Recently proposed variations of nested arrays called dilated nested arrays (DNA) and displaced DNA (DDNA) [12] are also used in comparisons. All these modifications of the nested array require two parameters N_1 and N_2 for construction. For a given total number of sensors, optimal values of N_1 and N_2 are used for each array. One key drawback of all these variations of nested arrays is that $w(2)$ of these arrays increases linearly with N_1 (and optimal N_1 is proportional to N).

We also include MRAs [2] in our comparison, but MRAs are available only for a limited number of sensors [2], [4]. In [3], the authors performed a restricted search for MRAs for $N \leq 20$ and tabulated the (approximate) MRAs they found using their restricted search. They also noted a general pattern of sensor locations in the arrays they obtained. The maximum inter-element spacing constraint (MISC) arrays [13] seem to be motivated by this general closed-form pattern noticed in [3]. In addition, the authors of [3] compiled another set of arrays, which we call constrained-MRAs (cMRA). These arrays maximize the ULA segment in the difference coarray under the constraint that $w(1) = 0$. The tabulated cMRAs in [3] are only an approximation to the ideal cMRAs because of the restricted search performed. As these arrays have $w(1) = 0$, they can effectively mitigate mutual coupling, as we will see in the simulations.

Out of several generalizations of coprime arrays (CPA) [6], we choose the following four in our comparisons. CADiS array [7] is generated by displacing and compressing one of the sparse ULAs of a coprime array. These arrays can have $w(l) = 0$ for several small values of l and hence can effectively mitigate mutual coupling, similar to the proposed arrays. However, as noted in Sec. I-B, the ULA segment in the difference coarray of CADiS does not start immediately after the few initial holes unlike the proposed arrays, and hence the maximum number of identifiable DOAs can be smaller than our proposed arrays as well will see. Furthermore, CADiS requires 3 design parameters (M, N, and p from [7] such that M and N are coprime and $p > 1$ divides M). For a given total number of sensors, or a fixed aperture, it is not easy to come up with optimal parameters that maximize the ULA segment in the coarray of CADiS, without enumerating all possibilities of design parameters (M, N, and p from [7]). Furthermore, for a certain number of sensors (such as 17, 23, and 29), there are no possible CADiS array constructions [14]. Another modification of coprime arrays we use for comparison is thinned coprime array (TCA) [14]. It has the same aperture and DOFs as the original coprime array but with fewer sensors and smaller coarray weights than the original coprime array. Four variations of padded coprime arrays (PCA) are proposed in [15] by characterizing hole locations in a tailored CADiS array and filling up those holes by augmenting a small number of additional sensors. Out of these, extended PCA (ePCA) has the longest ULA segment in the coarray. Impressively, ePCA (with parameters M and N from [15]) can achieve $w(l) = 1, 1 \leq l \leq M-1$ when M is odd. In some simulations, we also consider the enhanced and generalized coprime array (EGCA) [54], which can have a larger ULA segment in coarray and smaller mutual coupling than other variations of coprime arrays.

In Section VI-A, we compare the coarray properties for various arrays and illustrate coarray-MUSIC spectra obtained when estimating $D > N$ DOAs. We then conduct two types of Monte-Carlo simulations. The first set of simulations compares different arrays when the number of sensors N is fixed, and the array apertures can differ. The second set of simulations involves

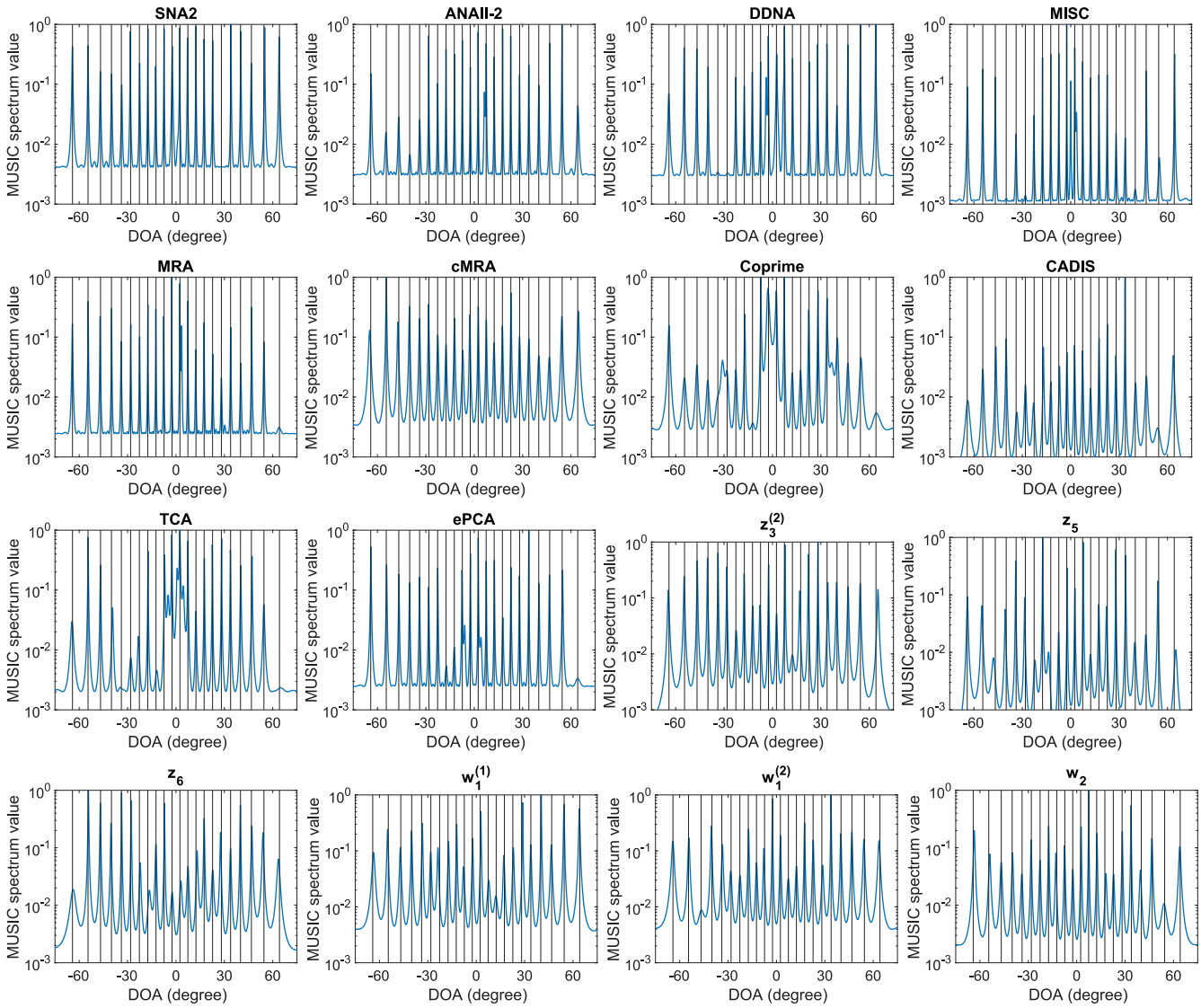

Fig. 2. Coarray-MUSIC spectra obtained when identifying $D = 22$ DOAs uniformly spaced in ω domain from -0.9π to 0.9π with different 16-sensor arrays from Table IV. SNR of 0 dB, mutual coupling with $c = 0.3$ and $B = 10$, and 100 snapshots are considered. Black vertical lines correspond to the true DOA locations. Except for CADiS and cMRA, all other arrays from the literature do not correctly identify all 22 DOAs and miss out on at least one DOA. On the other hand, the proposed arrays are able to identify all DOAs correctly with a small MSE by producing coarray-MUSIC spectra having peak locations close to each true DOA.

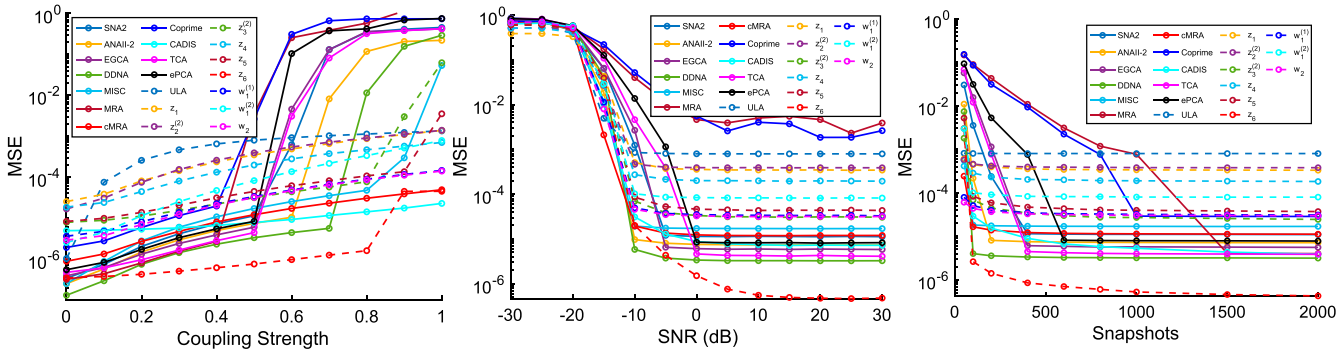

Fig. 3. MSE when estimating $D = 6$ DOAs uniformly spaced in ω from -0.8π to 0.8π with 16-sensor arrays. (a) SNR $= 5$ dB and $K = 500$, (b) $c = 0.5$ and $K = 500$, (c) $c = 0.5$ and SNR $= 5$ dB. Although many of the proposed arrays perform worse than other arrays from the literature, $\mathbf{z}_6$ is found to perform the best in most situations.

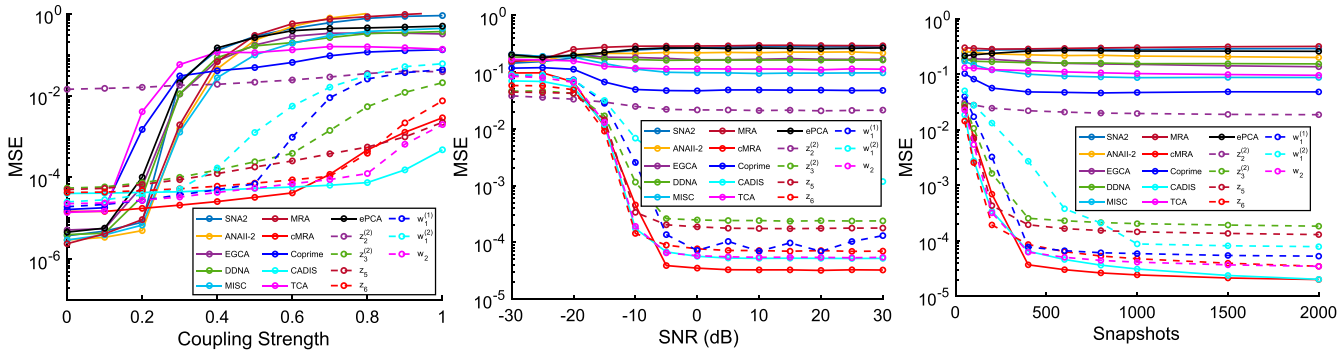

Fig. 4. MSE when estimating $D = 20$ DOAs uniformly spaced in ω from -0.9π to 0.9π with 16-sensor arrays. (a) SNR $= 5$ dB and $K = 500$, (b) $c = 0.5$ and $K = 500$, (c) $c = 0.5$ and SNR $= 5$ dB. Arrays with $w(1) = 0$ have smaller MSE, whereas arrays with $w(1) \neq 0$ cannot identify all the DOAs correctly, resulting in high MSE.

a fixed array aperture, while the number of sensors in arrays can vary. Each data point in the graphs is averaged over 1000 Monte-Carlo trials in every Monte-Carlo simulation. In these trials, the source amplitudes $\mathbf{s}[k]$ and noise realizations $\mathbf{n}[k]$ are randomly chosen according to the signal model described in Sec. II. All sources are assumed to have equal powers. To estimate DOAs with sparse arrays, we use the coarray root-MUSIC algorithm, as described in Sec. III, using the largest ULA segment (possibly one-sided) in the difference coarray. As for the ULA, we apply direct (i.e., using $\widehat{\mathbf{R}}_x$) root-MUSIC, as it usually performs better than coarray root-MUSIC [47], [48]. The DOA estimation mean squared error (MSE) is calculated in the ω domain as

$$\frac{1}{1000D}\sum_{q=1}^{1000}\sum_{i=1}^{D}(\omega_i - \hat{\omega}_{iq})^2, \tag{35}$$

where $\{\hat{\omega}_{iq}\}_{i=1}^{D}$ are the estimated DOA in the q-th Monte-Carlo trial. The mutual coupling model described in Eq. (9) is used with $B = 10$, $c_1 = ce^{j\pi/3}$, and $c_l = (c_1/l)e^{-j(l-1)\pi/8}$, where $|c_1| = c \in [0, 1]$, represents the coupling strength. These values for coupling coefficients have been used in most of the previous papers on sparse arrays [9], [12], [14], [15], and we use the same values in all our simulations here for consistency. In [24], it was noted that the DOA estimation performance may vary based on the phases of the coupling coefficients chosen. Further research is required to understand the effect of the phases of mutual coupling coefficients on DOA estimation.

A. Array Properties and Coarray-MUSIC Spectra

We now compare the coarray properties of the proposed arrays with the well-known arrays discussed in the previous subsection for a fixed number of sensors, $N = 16$. For nested array variations, array designs with optimal N_1 and N_2 that maximize the number of identifiable DOAs are chosen. Similarly, an optimal pair of coprime integers that maximize the number of identifiable DOAs is chosen for coprime array. The same design parameters are chosen for ePCA. Out of possible TCA configurations, we choose the array that can identify the most number of DOAs. Out of possible CADiS configurations, we choose the one with $w(l) = 0$ for $l = 1, 2$ for a fair comparison with the proposed arrays. Fig. 1 plots the coarray weights $w(l)$ for $0 \leq l \leq 40$. It is observed that although the proposed arrays have some large weights, the weights that contribute the most to the mutual coupling effect are either zero or relatively small. With fixed $N = 16$, each array has a different aperture A and the maximum number of identifiable DOAs using coarray root-MUSIC (D_m), as shown in Table IV. The proposed $\mathcal{O}(N)$ aperture arrays have a relatively smaller aperture and can identify fewer DOAs than $\mathcal{O}(N^2)$ aperture arrays. The coupling leakage values ($\mathcal{L}$) in Table IV are calculated with $c = 0.3$ and $B = 10$ (Eq. (10)). The coupling leakage is found to be smallest for $\mathbf{z}_6$, followed next by CADiS, $\mathbf{w}_2$, and $\mathbf{z}_5$. Coarray weights $w(l)$ for $1 \leq l \leq 5$ are also shown in the Table. Only the proposed arrays, CADiS, and cMRA have $w(1) = 0$. Although CADiS has a small mutual coupling, it can identify fewer DOAs compared to the proposed $\mathcal{O}(N^2)$ aperture arrays $\mathbf{w}_1^{(1)}$, $\mathbf{w}_1^{(2)}$, and $\mathbf{w}_2$.

Next, we consider the task of estimating $D = 22 (> N = 16)$ DOAs uniformly spaced in the ω domain from -0.9π to 0.9π with these arrays. SNR of 0 dB and 100 snapshots are considered. Note that ULA, $\mathbf{z}_1$, and $\mathbf{z}_2^{(2)}$, and $\mathbf{z}_4$ cannot identify 22 DOAs with coarray-MUSIC as they have $D_m < 22$. These arrays will be included in the comparisons in the next subsections for simulations with smaller D. Fig. 2 shows the coarray-MUSIC spectra obtained for the rest of the arrays. We observe that arrays that do not have $w(1) = 0$ do not produce correct peaks in the coarray-MUSIC spectra for some DOAs. On the other hand, the proposed arrays, CADiS, and cMRA can effectively mitigate the effect of mutual coupling and produce peaks in the coarray-MUSIC spectra corresponding to all 22 DOAs. The DOA estimation MSE is also small for these arrays with $w(1) = 0$, as shown in the last column of Table IV.

B. Monte-Carlo Simulations With a Fixed Number of Sensors

With the same set of arrays with $N = 16$ sensors, we perform Monte-Carlo simulations to compare DOA estimation performance. First, for the simulations in Fig. 3, we consider $D = 6$ DOAs spaced uniformly in the ω domain from -0.8π to 0.8π. We consider SNR of 5 dB, 500 snapshots, and coupling strength $c = 0.5$. Out of these three, we fix two quantities at a time and vary the third quantity to measure its impact on DOA

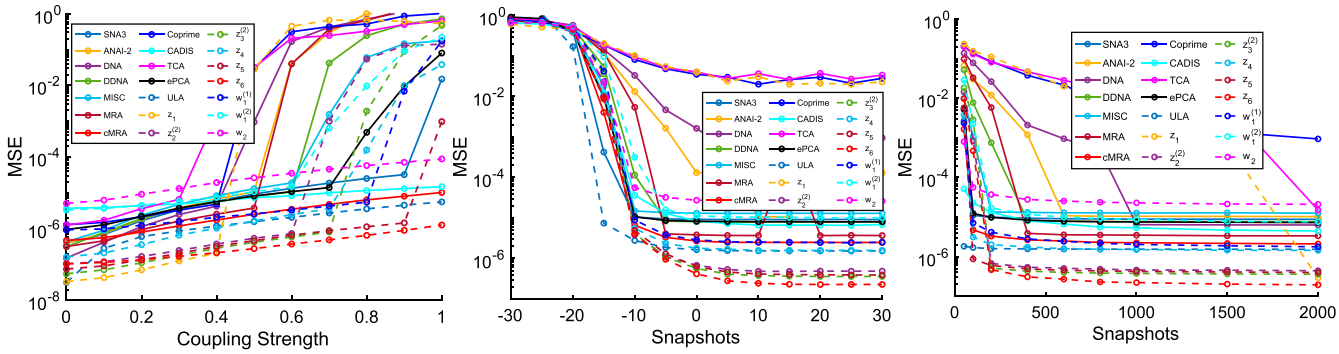

Fig. 5. MSE when estimating $D = 6$ DOAs spaced non-uniformly in ω domain with different arrays under aperture constraint $A \leq 100$ and $N \leq 50$. (a) SNR $= 5$ dB and $K = 500$, (b) $c = 0.5$ and $K = 500$, (c) $c = 0.5$ and SNR $= 5$ dB. The proposed $\mathcal{O}(N)$ aperture arrays perform much better than other sparse arrays as, under aperture constraint, they can fit in more sensors while maintaining small coupling leakage.

estimation error. We see that in this situation, with a relatively small number of sensors and few DOAs, many of the proposed arrays perform worse than the other sparse arrays. However, notably, $\mathbf{z}_6$ performs the best in this situation for a large range of c, SNR, and snapshots. Array $\mathbf{z}_6$ performs well because it has $w(1) = w(2) = 0$, and small $w(3)$ and $w(4)$, which makes it robust to the presence of high mutual coupling. In particular, in Fig. 3(a) we see that the increase in MSE for the proposed arrays is gradual as the coupling strength c is increased. In contrast, for most of the other arrays, MSE increases drastically as c increases beyond a certain point. The sudden increase in MSE usually indicates some of the DOAs being misidentified (similar to the case in Fig. 2). Despite having a smaller aperture and shorter ULA segment in coarray compared to the other $\mathcal{O}(N^2)$ aperture arrays, we see from Fig. 3(b) and 3(c) that $\mathbf{z}_6$ performs better when SNR is larger than 0 dB and more than 100 snapshots are used.

Next, we change the number of DOAs to $D = 20$ and repeat the above set of simulations. The DOAs are spaced uniformly from -0.9π to 0.9π in the ω domain. In Fig. 4 we see a clear separation between the arrays based on whether $w(1) = 0$ or not. Arrays with $w(1) = 0$ (irrespective of whether the aperture is $\mathcal{O}(N)$ or $\mathcal{O}(N^2)$) have smaller MSE than arrays for which $w(1) \neq 0$. The MSE for $\mathbf{z}_2^{(2)}$ is large because $D = 20$ DOAs is barely within the maximum number of identifiable DOAs (D_m) with this array (see Table IV). From Fig. 4(a) note that for $c \leq 0.2$, proposed arrays have larger MSE than most other arrays. For such small mutual coupling, the arrays with larger lengths of the ULA segment in coarray have smaller MSE. This indicates that for small mutual coupling, making $w(1) = 0$ to reduce mutual coupling is not as critical as it is when the high mutual coupling is present ($c > 0.2$). We see a similar ordering of arrays in Fig. 4(b) and 4(c). The MSEs saturated to a high value are indicative of misidentified DOAs. This simulation makes it clear that under high mutual coupling and for larger D, $w(1) = 0$ is required to correctly identify the DOAs.

C. Monte-Carlo Simulations Under Aperture Constraint

As we explained in the introduction, array design may be constrained by the available aperture, in practical applications.

TABLE V
PROPERTIES OF ARRAYS WHEN $A \leq 100$ AND $N \leq 50$. COUPLING LEAKAGE $\mathcal{L}$ IS CALCULATED WITH $c = 0.3$ AND $B = 10$. MANY OF THE PROPOSED $\mathcal{O}(N)$ APERTURE ARRAYS HAVE MORE SENSORS BUT SMALLER $\mathcal{L}$ COMPARED TO THE $\mathcal{O}(N^2)$ APERTURE ARRAYS FROM THE LITERATURE

Array	N	$\mathcal{L}$	D_m	Coarray Weights				
				w(1)	w(2)	w(3)	w(4)	w(5)
SNA3	19	0.1684	99	1	5	2	4	1
ANAII-2	17	0.2152	86	2	7	2	5	2
DNA	18	0.1909	89	1	8	1	6	1
DDNA	17	0.1692	80	1	5	1	3	1
MISC	17	0.1814	93	1	6	1	4	2
MRA	16	0.2299	90	4	2	1	1	3
cMRA	18	0.1722	48	0	8	2	7	2
Coprime	20	0.1757	59	2	2	2	2	11
CADiS	16	0.0712	25	0	0	0	0	6
TCA	17	0.1436	59	1	1	1	1	10
ePCA	18	0.1414	75	1	1	1	1	10
ULA	50	0.46	49	49	48	47	46	45
$\mathbf{z}_1$	50	0.2437	48	0	48	1	47	1
$\mathbf{z}_2^{(2)}$	34	0.1611	47	0	1	31	1	1
$\mathbf{z}_3^{(2)}$	27	0.1246	47	0	1	2	23	1
$\mathbf{z}_4$	33	0.157	45	0	0	30	1	1
$\mathbf{z}_5$	26	0.1179	44	0	0	2	22	1
$\mathbf{z}_6$	22	0.1031	43	0	0	3	1	17
$\mathbf{w}_1^{(1)}$	18	0.1801	44	0	8	5	7	1
$\mathbf{w}_1^{(2)}$	14	0.1649	27	0	6	1	5	1
$\mathbf{w}_2$	14	0.1088	25	0	0	5	1	3

To compare array performance under such practical constraints, we consider a situation where a maximum aperture of length 100 and a maximum of 50 sensors are available. For each array type under consideration, we appropriately choose the number of sensors such that the array satisfies the aperture constraint of 100. For example, a super nested array has 19 sensors, ULA and $\mathbf{z}_1$ have 50 sensors each, and $\mathbf{z}_3$ has 27 sensors. Table V shows the number of sensors, the maximum number of identifiable DOAs with coarray-MUSIC (D_m), coupling leakage ($\mathcal{L}$) calculated with $c = 0.3$, $B = 10$, and the first 5 coarray weights. Note that the proposed $\mathcal{O}(N)$ aperture arrays can fit more sensors in the available aperture than the $\mathcal{O}(N^2)$ aperture arrays from the literature and at the same time, have a smaller coupling leakage than many of those arrays (except CADiS, which has $w(l) = 0$ for $1 \leq l \leq 4$).

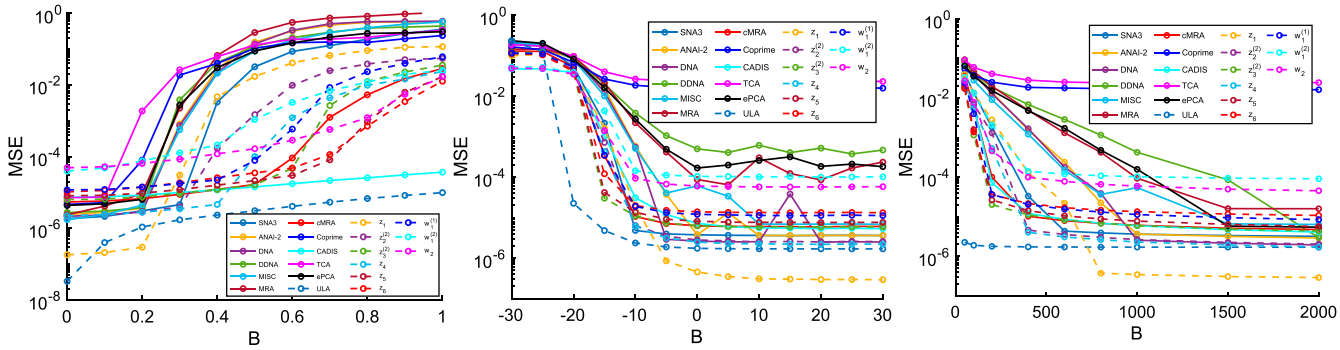

Fig. 6. MSE when estimating $D = 20$ DOAs uniformly spaced in ω from -0.9π to 0.9π with different arrays under aperture constraint $A \leq 100$ and $N \leq 50$. (a) SNR $= 5$ dB and $K = 500$, (b) $c = 0.3$ and $K = 1000$, (c) $c = 0.3$ and SNR $= 5$ dB. Despite high coupling leakage $\mathcal{L}$, ULA performs the best under low SNR or a small number of snapshots. The proposed array $\mathbf{z}_1$ performs well at higher SNRs or when a large number of snapshots are available. CADiS and ULA are found to perform well under very high mutual coupling.

In general, arrays with fewer sensors and sparser sensor arrangements can help minimize the impact of mutual coupling. However, a smaller number of sensors also means fewer observations per snapshot, which may result in less accurate DOA estimation. On the other hand, an array with a larger number of sensors provides more spatial samples of the impinging signals. But, under the aperture constraint, the sensors need to be closer to each other on average, which increases the effect of mutual coupling. Therefore, there is an interesting tradeoff in choosing the appropriate number of sensors and array geometry when the array aperture is constrained, and mutual coupling is present.

In Fig. 5, we examine the scenario with $D = 6$ DOAs located at $-0.8\pi, -0.35\pi, -0.1\pi, 0.05\pi, 0.4\pi, 0.8\pi$ in the ω domain. The DOAs are spaced non-uniformly unlike the other simulation examples. We compare the MSE of DOA estimation for different arrays constructed under the $A \leq 100$ and $N \leq 50$ constraints. We consider an SNR of 5 dB, coupling strength of $c =$ 0.5, and 500 snapshots, and vary one of these three quantities at a time to measure its impact on DOA estimation performance. Based on the results, we observe that the proposed $\mathcal{O}(N)$ aperture arrays perform significantly better than all other $\mathcal{O}(N^2)$ aperture arrays. In particular, from Fig. 5(a) it can be observed that $\mathcal{O}(N)$ aperture arrays perform better than other arrays even when $c = 0$ (i.e. when no mutual coupling is present). This is because $\mathcal{O}(N)$ aperture arrays have more sensors than $\mathcal{O}(N^2)$ aperture arrays under aperture constraint. From Fig. 5(b) and 5(c) it can be observed that for SNR larger than -10 dB and more than 100 snapshots, many of the proposed $\mathcal{O}(N)$ aperture sparse arrays perform better than other arrays.

Next, in Fig. 6, we consider $D = 20$ DOAs spaced uniformly in the ω domain from -0.9π to 0.9π. We consider the same arrays as in the previous simulation with $A \leq 100$ and $N \leq 50$. In Fig. 6(a), when $K = 500$ and SNR is 5 dB, ULA performs the best for most values of c despite its large coupling leakage and smaller aperture compared to the other arrays. A part of the reason for this may be that ULA has a large number of sensors and it uses direct root-MUSIC (and not coarray root-MUSIC). CADiS is also found to perform well for higher values of c. However, in Fig. 6(b), where $c = 0.3$ and $K = 1000$, we see that $\mathbf{z}_1$ can perform the best when the SNR is -5dB or more. In Fig. 6(c), where $c = 0.3$ and SNR $= 5$ dB, we observe that for more than 800 snapshots $\mathbf{z}_1$ can perform better than ULA. In Fig. 6(b) and 6(c), when SNR is less than -10 dB, or when fewer than 800 snapshots are used, ULA is observed to be better than other arrays despite having large coupling leakage.

D. Some Additional Simulations

The proposed weight-constrained nested arrays with $\mathcal{O}(N^2)$ aperture have an advantage when there is no aperture constraint, and a large number of DOAs need to be identified under high mutual coupling. This is demonstrated by the simulation in Fig. 7. Here, we consider arrays with $N = 25$ sensors. Note that cMRA [3] is not available for $N > 20$. Out of the possible CADiS array configurations for $N = 25$, we choose the array with $w(l) = 0$ for $1 \leq l \leq 4$ to reduce the mutual coupling effect. SNR of 5 dB, coupling strength $c = 0.3$, and 500 snapshots are considered. We vary the number of DOAs D and plot the MSE for different arrays. We can see that the proposed array $\mathbf{w}_2$ has the smallest MSE when $35 \leq D \leq 80$. Also, arrays $\mathbf{w}_1^{(1)}$, $\mathbf{w}_1^{(2)}$, and $\mathbf{w}_2$ can identify more DOAs than CADiS.

In Fig. 8, we also plot the MSE for the arrays from Table V (with $A \leq 100$ and $N \leq 50$) as the parameter B in the mutual coupling model is varied from 10 to 100. We observe that the general trend of the proposed arrays compared to existing arrays remains consistent as the parameter B is changed. This means that for different values of B, many of the proposed arrays can still perform better than the existing arrays.

As mentioned at the end of Sec. II-C, although coarray-based DOA estimation assumes uncorrelated sources, correlated sources can be present in practical situations. To evaluate the DOA estimation performance of the weight-constrained sparse arrays proposed in this paper for correlated sources, we conduct additional simulation experiments. Using the 16-sensor arrays from Table IV, 10 DOAs uniformly spaced in the ω-domain from -0.9π to 0.9π are estimated. Although when the sources are correlated, the ideal correlations do not have the sum of sinusoids form as in Eq. (12), we still estimate $\widehat{R}(l)$ as in Eq. (11) and construct the matrix by $\widehat{\mathbf{R}}$ from Eq. (13) to estimate DOAs. In Fig. 9, the correlation coefficient

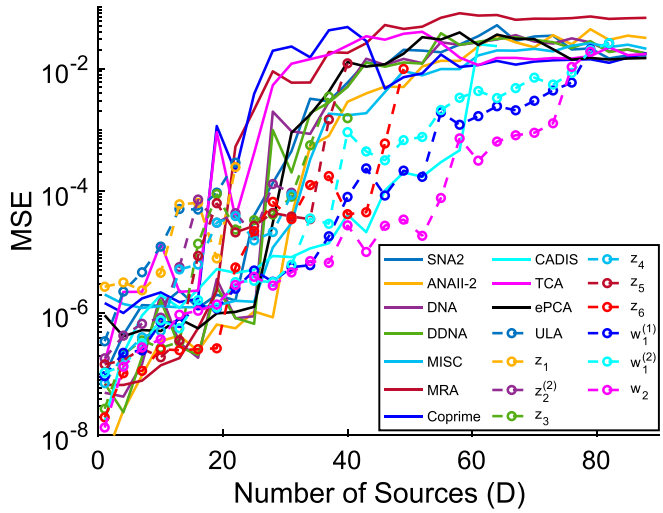

Fig. 7. MSE when identifying D DOAs spaced uniformly in the ω domain from -0.9π to 0.9π with 25-sensor arrays. SNR = 5 dB, $K = 500$, and $c = 0.3$. Array $\mathbf{w}_2$ has the smallest MSE when $35 \leq D \leq 80$. Arrays $\mathbf{w}_1^{(1)}$, $\mathbf{w}_1^{(2)}$, and $\mathbf{w}_2$ can identify more DOAs than CADiS.

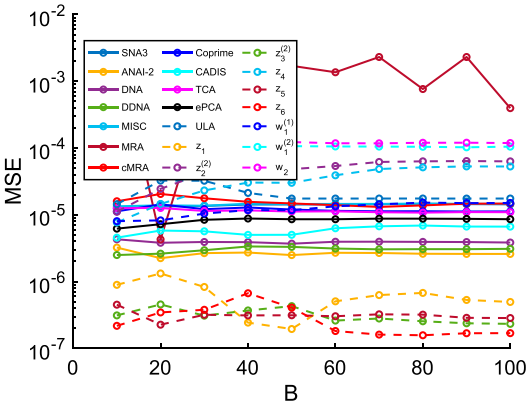

Fig. 8. MSE when identifying 6 DOAs spaced uniformly in the ω domain from -0.8π to 0.8π for arrays with $A \leq 100$ and $N \leq 50$. SNR = 5 dB, $K = 500$, and $c = 0.5$. The general trend of the proposed arrays compared to existing arrays remains consistent as the parameter B is changed.

between the second and fifth sources is set to $\rho e^{-j\pi/4}$, and the rest of the sources are uncorrelated. The magnitude of the correlation coefficient ρ is varied on the x-axis to measure its impact on DOA estimation MSE. We observe that in the absence of mutual coupling ($c = 0$), the rate of increase in MSE for most of the proposed arrays is not significantly different from the rate of increase in MSE for other sparse arrays. Moreover, in the presence of mutual coupling with $c = 0.4$, the proposed arrays still perform much better than other arrays from the literature, in the presence of a correlated source pair.

Next, in Fig. 10, we introduce a correlation coefficient of $\rho/2 \cdot e^{j\pi/3}$ between the seventh and ninth source, in addition to the correlation coefficient of $\rho e^{-j\pi/4}$ between the second and fifth source. Thus, there are now two correlated source pairs. These numerical results indicate that the proposed arrays can continue to perform well in the presence of high mutual coupling and high correlations between a few pairs of sources.

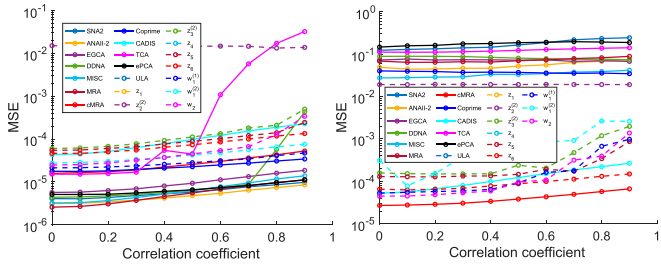

Fig. 9. MSE when estimating $D = 10$ DOAs uniformly spaced in ω from -0.9π to 0.9π with 16-sensor arrays when SNR = 5 dB, and $K = 500$. The correlation coefficient between the second and fifth source is taken to be $\rho e^{-j\pi/4}$. (a) $c = 0$, and (b) $c = 0.4$.

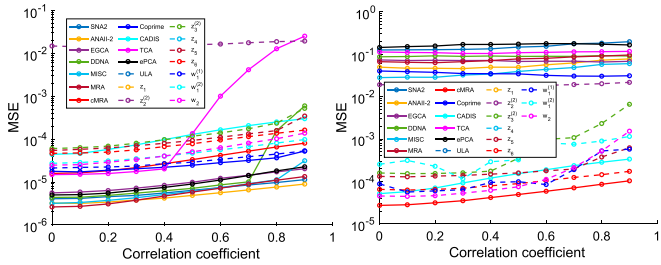

Fig. 10. MSE when estimating $D = 10$ DOAs uniformly spaced in ω from -0.9π to 0.9π with 16-sensor arrays when SNR = 5 dB, and $K = 500$. The correlation coefficient between the second and fifth source is taken to be $\rho e^{-j\pi/4}$, and the correlation coefficient between the seventh and ninth source is $\rho/2 \cdot e^{j\pi/3}$. (a) $c = 0$, and (b) $c = 0.4$.

E. Main Conclusions From Simulations

The observations from the above numerical simulations can be summarized as follows. These also serve as a guideline for the situations in which the proposed arrays can be used and can be expected to perform well.

For a fixed number of sensors: When $c > 0.2$ and D is large, arrays with $w(1) = 0$ or $w(1) = w(2) = 0$ are necessary to effectively mitigate the effect of mutual coupling, and correctly identify all DOAs (Figs. 2 and 4). Arrays with $w(1) \neq 0$ perform poorly in this setting. However, there is no advantage to using arrays with $w(1) = 0$ or $w(1) = w(2) = 0$ when $c < 0.2$. For a small number of DOAs, $\mathcal{O}(N)$ aperture array having small coarray weights (such as $\mathbf{z}_6$) can perform well (Fig. 3). Proposed arrays with $\mathcal{O}(N^2)$ aperture are suitable for identifying a large number of DOAs with smaller errors in the presence of mutual coupling (Fig. 7). The proposed arrays also continue to perform well when a few source pairs are correlated (Figs. 9 and 10).

Under aperture constraint: Under fixed aperture, the proposed $\mathcal{O}(N)$ aperture arrays can accommodate a larger number of sensors while still maintaining low coupling leakage (Table V). This makes them effective regardless of the mutual coupling strength when there are only a few DOAs (Fig. 5). For a larger number of DOAs, some of the proposed arrays (such as $\mathbf{z}_1$) can perform well provided a high SNR and a larger number of snapshots are available (Fig. 6). At low SNRs and for a small number of snapshots, ULA is found to perform the best despite having high coupling leakage.

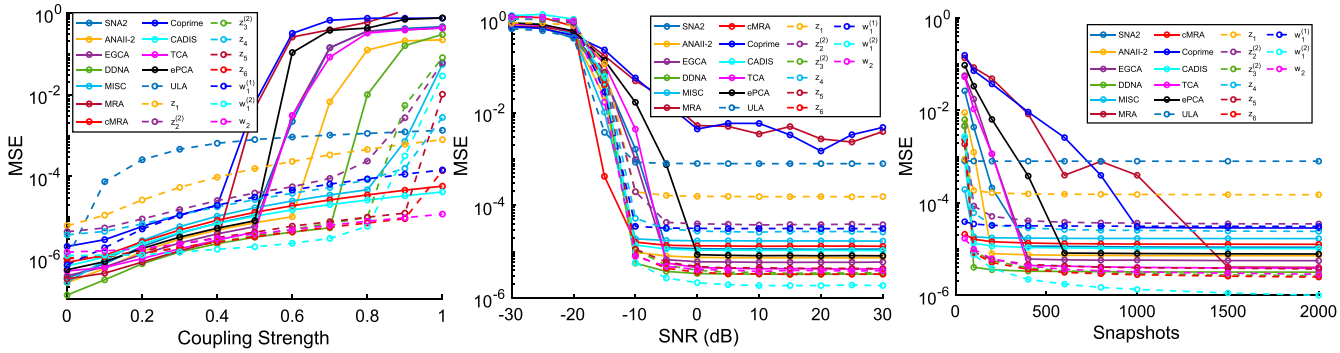

Fig. 11. MSE when estimating $D = 6$ DOAs uniformly spaced in ω from -0.8π to 0.8π with 16-sensor arrays using 'augmented root-MUSIC' [55]. (a) SNR $= 5$ dB and $K = 500$, (b) $c = 0.5$ and $K = 500$, (c) $c = 0.5$ and SNR $= 5$ dB. These plots are analogous to the plots from Fig. 3. We observe here that because of the use of both ULA segments present in the coarrays of weight-constrained sparse arrays, now many of the proposed arrays can perform at par or better than other arrays from the literature.

F. Further Enhancing the Performance of Proposed Weigh-Constrained Sparse Arrays

Note that all the simulations in this section are based on coarray root-MUSIC. We chose coarray root-MUSIC because it has theoretical identifiability guarantees under ideal conditions, is conceptually simple to use, and does not require hyperparameter tuning like some other methods (such as dictionary-based methods) do. However, because of the DOA estimation algorithm based on a one-sided coarray segment, the proposed arrays are at a "disadvantage" compared to the arrays having a *central* ULA segment in the coarray. For the arrays with *central* ULA segment in the coarray, both sides of the coarray are used to form the matrix $\widehat{\mathbf{R}}$, whereas, for the arrays with central holes in their coarray (i.e., $w(1) = 0$), only one side of the coarray is used. Despite this limitation, the proposed arrays have a smaller MSE compared to previous arrays in the literature in the presence of mutual coupling under several simulation settings. This already demonstrates the value of our proposed arrays.

However, to further enhance the performance of the proposed arrays, other DOA estimation algorithms that can use both sides of the difference coarray should be considered in the future. In our upcoming work [55], we propose 'augmented root-MUSIC' that can utilize the ULA segments on both sides of the coarrays with central holes. We have found that for some of the proposed arrays, the augmented root-MUSIC can have over an order of magnitude smaller MSE than coarray root-MUSIC that uses a one-sided ULA segment. The basic idea is to stack the Toeplitz matrices formed from the ULA segments in the coarray from positive sides and negative sides. Then, a 'noise subspace' in a much higher dimension is estimated using the SVD of the augmented matrix. The details will be explained in [55]. Here we provide one simulation example to demonstrate its advantage.

We rerun the simulations from Fig. 3 using the augmented root-MUSIC algorithm [55]. The resulting plots are shown in Fig. 11. Note that in Fig. 3, only array $\mathbf{z}_6$ performed better than other arrays from the literature. Whereas in Fig. 11 above using augmented root-MUSIC, many of the proposed arrays now have over an order of magnitude smaller MSE than earlier and perform at par or better than arrays from the literature. As another future direction, the central holes in the coarrays can be filled using appropriate coarray interpolation techniques [56], [57], [58]. However, it can be challenging to incorporate mutual coupling into such algorithms. Once the central holes are appropriately filled through interpolation, we can use the central ULA segment in coarray instead of the one-sided segment. These directions will be explored in our future work.

VII. Concluding Remarks

In this paper, we introduced new weight-constrained sparse arrays that are robust to the presence of high mutual coupling. We argued that with a large number of sensors N, we may not always require $\mathcal{O}(N^2)$ degrees of freedom, and $\mathcal{O}(N^2)$ length aperture of such sparse arrays can be impractical for various applications. To better accommodate aperture constraints and high mutual coupling, we proposed two modifications to the array design criteria and presented several $\mathcal{O}(N)$ aperture arrays with either $w(1) = 0$ or $w(1) = w(2) = 0$. Many of these arrays can still identify $D > N$ DOAs (such as $D = 2N$) using coarray-MUSIC on a one-sided ULA segment present in the coarray. These arrays are obtained by appropriately dilating a ULA and augmenting it with a few additional sensors. Through Monte-Carlo simulations, we demonstrated that these new arrays can outperform existing arrays from the literature under high mutual coupling or aperture constraint conditions. Additionally, we proposed another type of arrays with $w(1) = 0$ or $w(1) = w(2) = 0$ and $\mathcal{O}(N^2)$ aperture, called weight-constrained nested arrays, which are suitable for identifying a large number of DOAs under high mutual coupling when aperture is not constrained.

The theme of an 'aperture-aware' array design introduced in this work can be further explored to design sparse arrays systematically under aperture constraints. Several interesting array design questions arise under such a setting. For example, given a fixed aperture A and a fixed number of sensors $N < A$, it would be of interest to know the sensor arrangement that leads to the lowest mutual coupling and gives the best DOA estimation performance. Furthermore, similar to the 1D

weight-constrained sparse arrays introduced in this paper, 2D sparse arrays that have zero coarray weights at smaller lags are also of interest for future research.

ACKNOWLEDGEMENT

The authors wish to thank Po-Chih Chen for the discussion about the sparse arrays proposed in this work and for pointing out redundancy in an earlier construction of $\mathbf{w}_2$, which helped in making the design of $\mathbf{w}_2$ more economical.

REFERENCES

[1] H. Krim and M. Viberg, "Two decades of array signal processing research: The parametric approach," *IEEE Signal Proc. Mag.*, vol. 13, no. 4, pp. 67–94, Jul. 1996.

[2] A. Moffet, "Minimum-redundancy linear arrays," *IEEE Trans. Antennas Propag.*, vol. 16, no. 2, pp. 172–175, Mar. 1968.

[3] M. Ishiguro, "Minimum redundancy linear arrays for a large number of antennas," *Radio Sci.*, vol. 15, no. 6, pp. 1163–1170, 1980.

[4] F. Schwartau, Y. Schröder, L. Wolf, and J. Schoebel, "Large minimum redundancy linear arrays: Systematic search of perfect and optimal rulers exploiting parallel processing," *IEEE Open J. Antennas Propag.*, vol. 2, pp. 79–85, 2021.

[5] P. Pal and P. P. Vaidyanathan, "Nested arrays: A novel approach to array processing with enhanced degrees of freedom," *IEEE Trans. Signal Process.*, vol. 58, no. 8, pp. 4167–4181, Aug. 2010.

[6] P. P. Vaidyanathan and P. Pal, "Sparse sensing with co-prime samplers and arrays," *IEEE Trans. Signal Process.*, vol. 59, no. 2, pp. 573–586, Feb. 2011.

[7] S. Qin, Y. D. Zhang, and M. G. Amin, "Generalized coprime array configurations for direction-of-arrival estimation," *IEEE Trans. Signal Process.*, vol. 63, no. 6, pp. 1377–1390, Mar. 2015.

[8] M. Yang, L. Sun, X. Yuan, and B. Chen, "Improved nested array with hole-free DCA and more degrees of freedom," *Electron. Lett.*, vol. 52, no. 25, pp. 2068–2070, Dec. 2016.

[9] C.-L. Liu and P. P. Vaidyanathan, "Super nested arrays: Linear sparse arrays with reduced mutual coupling—Part I: Fundamentals," *IEEE Trans. Signal Process.*, vol. 64, no. 15, pp. 3997–4012, Aug. 2016.

[10] C.-L. Liu and P. P. Vaidyanathan, "Super nested arrays: Linear sparse arrays with reduced mutual coupling—Part II: High-order extensions," *IEEE Trans. Signal Process.*, vol. 64, no. 16, pp. 4203–4217, Aug. 2016.

[11] J. Liu, Y. Zhang, Y. Lu, S. Ren, and S. Cao, "Augmented nested arrays with enhanced DOF and reduced mutual coupling," *IEEE Trans. Signal Process.*, vol. 65, no. 21, pp. 5549–5563, Nov. 2017.

[12] A. M. Shaalan, J. Du, and Y.-H. Tu, "Dilated nested arrays with more degrees of freedom (DOFs) and less mutual coupling—Part I: The fundamental geometry," *IEEE Trans. Signal Proc.*, vol. 70, pp. 2518–2531, 2022, doi: 10.1109/TSP.2022.3174451.

[13] Z. Zheng, W.-Q. Wang, Y. Kong, and Y. D. Zhang, "MISC array: A new sparse array design achieving increased degrees of freedom and reduced mutual coupling effect," *IEEE Trans. Sig. Proc.*, vol. 67, no. 7, pp. 1728–1741, Apr. 2019.

[14] A. Raza, W. Liu, and Q. Shen, "Thinned coprime array for second-order difference co-array generation with reduced mutual coupling," *IEEE Trans. Signal Process.*, vol. 67, no. 8, pp. 2052–2065, Apr. 2019.

[15] W. Zheng, X. Zhang, Y. Wang, J. Shen, and B. Champagne, "Padded coprime arrays for improved DOA estimation: Exploiting hole representation and filling strategies," *IEEE Trans. Signal Process.*, vol. 68, pp. 4597–4611, 2020.

[16] R. Schmidt, "Multiple emitter location and signal parameter estimation," *IEEE Trans. Antennas Propag.*, vol. 34, no. 3, pp. 276–280, Mar. 1986.

[17] C.-L. Liu and P. P. Vaidyanathan, "Remarks on the spatial smoothing step in coarray MUSIC," *IEEE Signal Process. Lett.*, vol. 22, no. 9, pp. 1438–1442, Sep. 2015.

[18] R. Roy and T. Kailath, "ESPRIT-estimation of signal parameters via rotational invariance techniques," *IEEE Trans. Acoust., Speech, Signal Process.*, vol. 37, no. 7, pp. 984–995, Jul. 1989.

[19] R. Zhang, B. Shim, and W. Wu, "Direction-of-arrival estimation for large antenna arrays with hybrid analog and digital architectures," *IEEE Trans. Signal Process.*, vol. 70, pp. 72–88, 2022.

[20] L. Lu, G. Y. Li, A. L. Swindlehurst, A. Ashikhmin, and R. Zhang, "An overview of massive MIMO: Benefits and challenges," *IEEE J. Sel. Topics signal Process.*, vol. 8, no. 5, pp. 742–758, Oct. 2014.

[21] T. Svantesson, "Mutual coupling compensation using subspace fitting," in *Proc. IEEE Sensor Array Multichannel Signal Process. Workshop,* Piscataway, NJ, USA: IEEE Press, 2000, pp. 494–498.

[22] T. Svantesson, "Modeling and estimation of mutual coupling in a uniform linear array of dipoles," in *Proc. IEEE Int. Conf. Acoust., Speech Signal Process. (ICASSP)*, 1999.

[23] J. Shi, G. Hu, X. Zhang, and H. Zhou, "Generalized nested array: Optimization for degrees of freedom and mutual coupling," *IEEE Commun. Lett.*, vol. 22, no. 6, pp. 1208–1211, Jun. 2018.

[24] P. Kulkarni and P. P. Vaidyanathan, "Sparse, weight-constrained arrays with $O(N)$ aperture for reduced mutual coupling," in *Proc. IEEE Int. Conf. Acoust., Speech, Signal Proc.*, 2024, pp. 12891–12895.

[25] H. L. Van Trees, *Optimum Array Processing: Part IV of Detection, Estimation, and Modulation Theory*. Hoboken, NJ, USA: Wiley, 2004.

[26] A. Barabell, "Improving the resolution performance of eigenstructure-based direction-finding algorithms," in *Proc. IEEE Int. Conf. Acoust., Speech Signal Process. (ICASSP)*, 1983, pp. 336–339.

[27] P. Stoica and A. Nehorai, "MUSIC, maximum likelihood, and Cramer-Rao bound," *IEEE Trans. Acc., Speech, Signal Process.*, vol. 37, no. 5, pp. 720–741, May 1989,.

[28] P. Stoica and A. Nehorai, "Performance study of conditional and unconditional direction-of-arrival estimation," *IEEE Trans. Acoust., Speech, Sig. Proc.*, vol. 38, no. 10, pp. 1783–1795, Oct. 1990.

[29] B. D. Rao and K. S. Hari, "Performance analysis of root-MUSIC," *IEEE Trans. Acoust., Speech, Signal Process.*, vol. 37, no. 12, pp. 1939–1949, Dec. 1989.

[30] B. Friedlander and A. J. Weiss, "Direction finding in the presence of mutual coupling," *IEEE Trans. Antennas Propag.*, vol. 39, no. 3, pp. 273–284, Mar. 1991.

[31] E. BouDaher, F. Ahmad, M. G. Amin, and A. Hoorfar, "Mutual coupling effect and compensation in non-uniform arrays for direction-of-arrival estimation," *Digital Signal Process.*, vol. 61, pp. 3–14, Feb. 2017.

[32] F. Sellone and A. Serra, "A novel online mutual coupling compensation algorithm for uniform and linear arrays," *IEEE Trans. Signal Process.*, vol. 55, no. 2, pp. 560–573, Feb. 2007.

[33] Z. Ye, J. Dai, X. Xu, and X. Wu, "DOA estimation for uniform linear array with mutual coupling," *IEEE Trans. Aerosp. Electron. Syst.*, vol. 45, no. 1, pp. 280–288, Jan. 2009.

[34] C. A. Balanis, *Antenna Theory: Analysis and Design*. Hoboken, NJ, USA: Wiley, 2016.

[35] H.-S. Lui, H. T. Hui, and M. S. Leong, "A note on the mutual-coupling problems in transmitting and receiving antenna arrays," *IEEE Antennas Propag. Mag.*, vol. 51, no. 5, pp. 171–176, Oct. 2009.

[36] G. Brown, "Directional antennas," *Proc. Inst. Radio Eng.*, vol. 25, no. 1, pp. 78–145, 1937.

[37] H. King, "Mutual impedance of unequal length antennas in echelon," *IRE Trans. Antennas Propag.*, vol. 5, no. 3, pp. 306–313, Jul. 1957.

[38] K. M. Pasala and E. M. Friel, "Mutual coupling effects and their reduction in wideband direction of arrival estimation," *IEEE Trans. Aerosp. Electron. Syst.*, vol. 30, no. 4, pp. 1116–1122, Oct. 1994.

[39] I. Gupta and A. Ksienski, "Effect of mutual coupling on the performance of adaptive arrays," *IEEE Transact. Antennas Propag.*, vol. 31, no. 5, pp. 785–791, Sep. 1983.

[40] H. Hui, "Improved compensation for the mutual coupling effect in a dipole array for direction finding," *IEEE Trans. Antennas Propag.*, vol. 51, no. 9, pp. 2498–2503, Sep. 2003.

[41] H. S. Lui, H. T. Hui, "Mutual coupling compensation for direction-of-arrival estimations using the receiving-mutual-impedance method," *Int. J. Antennas Propag.*, vol. 2010, Mar. 2010, Art. no. 373061.

[42] R. P. Feynman, R. B. Leighton, and M. Sands, *The Feynman Lectures on Physics*, Vol. I the New Millennium Ed.: Mainly Mechanics, Radiation, and Heat. New York, NY, USA: Basic Books, 2011.

[43] S. Ramo, J. R. Whinnery, and T. Van Duzer, *Fields and Waves in Communication Electronics*. Hoboken, NJ, USA: Wiley, 1994.

[44] B. Friedlander, "On the mutual coupling matrix in array signal processing," in *Proc. 54th Asilomar Conf. Signals, Syst., Comput.*, 2020, pp. 1245–1249.

[45] Z. Yang and K. Wang, "Nonasymptotic performance analysis of direct-augmentation and spatial-smoothing ESPRIT for localization of more sources than sensors using sparse arrays," *IEEE Trans. Aerosp. Electron. Syst.*, vol. 59, no. 6, pp. 9379–9389, Dec. 2023.

[46] C.-L. Liu and P. Vaidyanathan, "Cramér–Rao bounds for coprime and other sparse arrays, which find more sources than sensors," *Digital Signal Process.*, vol. 61, pp. 43–61, Feb. 2017.
[47] M. Wang and A. Nehorai, "Coarrays, MUSIC, and the Cramér–Rao bound," *IEEE Trans. Signal Process.*, vol. 65, no. 4, pp. 933–946, Feb. 2017.
[48] P. Kulkarni and P. P. Vaidyanathan, "On the efficiency of coarray-based direction of arrival estimation," in *Proc. Asilomar Conf. Signals, Syst. Comput.,* Piscataway, NJ, USA: IEEE Press, 2023, pp. 1334–1338.
[49] S. Sedighi, B. S. M. R. Rao, and B. Ottersten, "An asymptotically efficient weighted least squares estimator for co-array-based DoA estimation," *IEEE Trans. Signal Process.*, vol. 68, pp. 589–604, 2020.
[50] Z. Zheng, Y. Huang, W.-Q. Wang, and H. C. So, "Augmented covariance matrix reconstruction for DOA estimation using difference coarray," *IEEE Trans. Signal Process.*, vol. 69, pp. 5345–5358, 2021.
[51] P. Sarangi, M. C. Hücümenoğlu, and P. Pal, "Beyond coarray MUSIC: Harnessing the difference sets of nested arrays with limited snapshots," *IEEE Signal Process. Lett.*, vol. 28, pp. 2172–2176, 2021.
[52] Z. Yang, X. Chen, and X. Wu, "A robust and statistically efficient maximum-likelihood method for DOA estimation using sparse linear arrays," *IEEE Trans. Aerosp. Electron. Syst.*, vol. 59, no. 5, pp. 6798–6812, Oct. 2023.
[53] Y. D. Zhang, M. G. Amin, and B. Himed, "Sparsity-based DOA estimation using co-prime arrays," in *Proc. IEEE Int. Conf. Acoust., Speech Signal Process.,* Piscataway, NJ, USA: IEEE Press, 2013, pp. 3967–3971.
[54] J. Shi, F. Wen, Y. Liu, Z. Liu, and P. Hu, "Enhanced and generalized coprime array for direction of arrival estimation," *IEEE Trans. Aerosp. Electron. Syst.*, vol. 59, no. 2, pp. 1327–1339, Apr. 2023.
[55] P. Kulkarni and P. P. Vaidyanathan, "Efficient use of non-central ULA segments in the coarrays of weight-constrained sparse arrays," submitted for publication.
[56] C.-L. Liu, P. Vaidyanathan, and P. Pal, "Coprime coarray interpolation for DOA estimation via nuclear norm minimization," in *Proc. IEEE Int. Symp. Circuits Syst. (ISCAS),* Piscataway, NJ, USA: IEEE Press, 2016.
[57] H. Qiao and P. Pal, "Unified analysis of co-array interpolation for direction-of-arrival estimation," in *Proc. IEEE Int. Conf. Acoust., Speech Signal Process. (ICASSP),* Piscataway, NJ, USA: IEEE Press, 2017, pp. 3056–3060.
[58] C. Zhou, Z. Shi, Y. Gu, and Y. D. Zhang, "Coarray interpolation-based coprime array DOA estimation via covariance matrix reconstruction," in *Proc. IEEE Int. Conf. Acoust., Speech Signal Process. (ICASSP)*, Piscataway, NJ, USA: IEEE Press, 2018.

Pranav Kulkarni (Student Member, IEEE) was born in 1997. He received the B.Tech. degree in electrical engineering with a minor in computer science from Indian Institute of Technology (IIT), Bombay, in 2019, and the master's degree in electrical engineering from California Institute of Technology (Caltech), in 2021. He is currently working toward the Ph.D. degree in digital signal processing with Caltech. His research interests include periodicity analysis, array signal processing, and line spectrum estimation. He was the recipient of first place in the Student Paper Contest at the 2022 Asilomar Conference on Signals, Systems, and Computers.

P. P. Vaidyanathan (Life Fellow, IEEE) received the B.Sc., B.Tech., and M.Tech. degrees from the University of Calcutta, Kolkata, India, in 1974, 1977, and 1979, respectively, and the Ph.D. degree in electrical and computer engineering from the University of California, Santa Barbara, CA, USA, in 1982. He is the Kiyo and Eiko Tomiyasu Professor of electrical engineering with California Institute of Technology (Caltech), Pasadena, CA, USA. He was the recipient of the IEEE CAS Society Golden Jubilee Medal, the Terman Award of the ASEE, the IEEE Gustav Robert Kirchhoff Technical Field Award in 2016, and the IEEE Signal Processing Society Technical Achievement Award in 2002, the Education Award in 2012, and the Society Award in 2016. He was the recipient of the EURASIP Athanasios Papoulis Award in 2021, a Foreign Fellow of the Indian National Academy of Engineering, and a member of the European Academy of Sciences and Arts. He was also the recipient of multiple awards for teaching with Caltech, including the Northrop Grumman Teaching Prize. He is the recipient of the IEEE Jack S. Kilby Signal Processing Medal and a member of the U.S. National Academy of Engineering.